UCRL 10129

# University of California

# Ernest O. Lawrence Radiation Laboratory



## SEARCH FOR MULTIPION RESONANCES IN THE REACTION $\bar{p} + p \rightarrow 3\pi^+ + 3\pi^- + n\pi^0$

Berkeley, California

## DISCLAIMER

Research and Development

UCRL-10129
UC-34 Physics
TID-4500 (17th Ed.)

UNIVERSITY OF CALIFORNIA
Lawrence Radiation Laboratory
Berkeley, California

Contract No. W-7405-eng-48

# SEARCH FOR MULTIPION RESONANCES IN THE REACTION $\bar{p} + p \rightarrow 3\pi^+ + 3\pi^- + n\pi^0$

Nguyen-Huu Xuong
(Thesis)

March 21, 1962

# SEARCH FOR MULTIPION RESONANCES IN THE REACTION $\bar{p}+p \rightarrow 3\pi^+ + 3\pi^- + n\pi^0$

Contents

Contents (cont.)

# SEARCH FOR MULTIPION RESONANCES IN THE REACTION $\bar{p} + p \rightarrow 3\pi^+ + 3\pi^- + n\pi^0$

Nguyen-Huu Xuong

Lawrence Radiation Laboratory
University of California
Berkeley, California

March 21, 1962

## Abstract

We report here the study of the reaction $\bar{p} + p \rightarrow 3\pi^+ + 3\pi^- + n\pi^0$ at 1.61 Bev/c ($E_{c.m.} = 2.290$ Bev), with the aim of detecting multipion resonances in the final states.

The experiment was performed in the Lawrence Radiation Laboratory's 72-inch liquid hydrogen bubble chamber. The total number of 6-prong events in the sample is 715. The events were measured with the Franckenstein measuring projector. The events were analyzed by using the PANG, KICK, and EXAMIN programs with IBM 704, 709, and 7090 computers.

The cross sections of various processes are found to be

$\sigma(\bar{p} + p \rightarrow 3\pi^+ + 3\pi^-) = 1.16 \pm .1$ mb,

$\sigma(\bar{p} + p \rightarrow 3\pi^+ + 3\pi^- + \pi^0) = 1.8 \pm .25$ mb,

$\sigma(\bar{p} + p \rightarrow 3\pi^+ + 3\pi^- + 2\pi^0) = 1.05 \pm .25$ mb.

The angular distributions are symmetrical for all three types of events.

The existence of the $\omega$ meson (T = 0, 3-pion resonance at 780 Mev) is further confirmed. With the hypothesis of G-parity conservation in the decay process (strong decay), the spin and parity of the $\omega$ meson is confirmed as $1^-$ by the Dalitz plot method. Even with the hypothesis of G-parity nonconservation in the decay process (electromagnetic decay), the $1^-$ spin-parity assignment is still strongly suggested by the small values of the ratios of $R[(\omega \rightarrow 4\pi)/(\omega \rightarrow \pi^+\pi^-\pi^0)]$ and $R[(\omega \rightarrow \text{neutral})/(\omega \rightarrow \pi^+ + \pi^- + \pi^0)]$. We do not observe any T = 0, 3-pion resonance at 550 Mev ($\eta$ meson).

The neutral four-pion effective mass $M_4$ distribution shows a suggestive but inconclusive peak at 1.04 Bev

The distribution of the 2-pion effective mass $M_2$ of the $\bar{p} + p \rightarrow 3\pi^+ + 3\pi^-$ events shows a big difference between $|Q| = 2$ (for like-pion pairs) and $Q = 0$ (for unlike-pion pairs) at the low-value region of $M_2$. At this region the $M_2$ distribution of like pion pairs lies above that from phase-space calculations, and the one of unlike-pion pairs is well below. We tentatively attribute this effect to the Bose-Einstein effect on the pions.

The ratio $R[(\rho^{\pm} \rightarrow \pi^{\pm} + \eta$ followed by $\eta \rightarrow \pi^+\pi^-\pi^0)/(\rho^{\pm} \rightarrow \pi^{\pm}\pi^0)]$ is determined to be $1.2 \pm 2.0\%$. This small ratio agrees with a $0^{-+}$ assignment for spin, parity and G parity of the $\eta$ meson, but cannot rule out the $1^{--}$ possibility. Upper limit of some other decay rates of $\rho$ and $\omega$ mesons are presented.

# I. INTRODUCTION

It is a little paradoxical that a search for more resonances or unstable particles can be introduced by a theory that tries to reduce the fundamental particles to three: the "Eightfold Way" Theory.[1]

In this theory Gell-Mann, using the Sakata Model[2] with only three fundamental particles p, n, $\Lambda$ (and their antiparticles $\bar{p}$, $\bar{n}$, $\bar{\Lambda}$), and supposing that mesons are formed of fundamental baryons and their antiparticles interacting via a "gluon," predicts the existences of two sets of mesons, the pseudoscalar set of $0^-$ mesons (spin = 0, parity odd) and the vector set of $1^-$ mesons (spin 1, parity odd). Each set is divided into a singlet and an octet. He also conjectures the existence of the scalar $0^+$ and $1^+$ axial-vector mesons. These mesons are shown in Table I.

Table I. Mesons proposed in the "Eightfold Way" Theory

A pseudoscalar octet would be composed of $3\,\pi$ ($\pi^+$, $\pi^0$, $\pi^-$), $2\,K$ ($K^+$, $K^0$), $2\,\bar{K}$ ($\bar{K}^0$, $K^-$), and $1\,\chi^0$.)

| Unitary Spin | I | S | PS($0^-$) | V($1^-$) | S($0^+$) | A($1^+$) |
|---|---|---|---|---|---|---|
| OCTET | 1 | 0 | $\pi$ | $\rho$ | $\pi'$ | $\rho'$ |
| | 1/2 | +1 | K | M | K' | M' |
| | 1/2 | -1 | $\bar{K}$ | $\bar{M}$ | $\bar{K}'$ | $\bar{M}'$ |
| | 0 | 0 | $\chi^0$ | $\omega$ | $\chi^{0'}$ | $\omega'$ |
| Singlet | 0 | 0 | A | B | A' | B' |

The decay of these proposed particles is governed by the conservation laws of strong (or electromagnetic) interactions. Here we are mostly interested in nonstrange particles (S = 0). Table II shows the prediction of the decays of these particles.

Table II. Prediction of decay of some proposed mesons with strangeness S = 0.[a]

| Particle | G parity | Strong decay | Electromagnetic decay |
|---|---|---|---|
| $\rho$ | +1 | $\pi^+\pi^0, \pi^+\pi^-, \pi^-\pi^0$ | |
| $\omega$, B | -1 | $\pi^+\pi^-\pi^0$ | $\pi^0\gamma$ |
| $\chi$, A | +1 | $4\pi$ | $3\pi, \pi^+\pi^-\gamma, 2\gamma$ |
| $\pi'$ | -1 | $5\pi, \bar{K}K, \chi^0\pi$ | $2\pi\gamma, 4\pi$ |
| $\rho'$ | -1 | $3\pi$ | $\pi\gamma$ |
| $\omega'$, $B'$ | +1 | $4\pi$ | $\pi^+\pi^-\gamma, 3\pi$ |
| $\chi'$, $A'$ | +1 | $\pi^+\pi^-, \pi^0\pi^0$ | $2\gamma$ |

a. See Appendix 1

In the vector theory of strong interactions Sakurai predicts the existence of three vector mesons: one with isotopic spin 1 corresponding to the $\rho$ and coupled to the isotopic spin current; two with isotopic spin 0, of which the heavier, corresponding to B in the Gell-Mann notation, is coupled to hypercharge current and the lighter $\omega$ to the baryonic current.[3]

The $\chi^0$ has also been predicted by many theorists.[4]

The existence of the $\rho$ meson has much more theoretical basis due to the calculations by Chew et al., by Federbush et al., and especially by Fraser and Fulco on the isovector form factor of the nucleon.[5] The existence of the $\omega$ meson is suggested by Nambu to explain the isoscalar form factor of the nucleon.[6]

Here we propose to search for these mesons in the reaction $\bar{p} + p \rightarrow 3\pi^+ + 3\pi^- + n\pi^0$ by calculating the effective mass of two, three, four and five pions, to study their distribution to see if they show any striking peaks, and to try to identify these peaks with the proposed decay mesons.

## II. ANTIPROTON BEAM

### Beam Design and Performance

We use pictures of the 72-inch hydrogen bubble chamber with a beam of antiprotons of 1.61 Bev/c. The design of the "separated" beam was patterned after the 1.17-Bev/c K beam of Eberhard, Good, and Ticho.[7] The details of the beam have been described elsewhere,[8] accordingly only an outline is given here, and a summary Table prescribed (Table III).

A schematic diagram of the beam setup is shown in Fig. 1.

The $\bar{p}$ beam was separated from the much more copious kaon, pion, and muon flux by means of three separator systems. Each system consists basically of two magnetic quadrupole lenses (triplet), one parallel-plate velocity spectrometer, and one slit (see Figs. 2 and 3).

The negative particles were extracted from the target inside the Bevatron through a hole in the magnet yoke. The final momentum interval accepted was defined by using the first quadrupole to focus the beam in the horizontal plane at the second quadrupole. Because of the initial momentum dispersion due to the Bevatron field, different momenta are focused at different points along a line normal to the beam direction. Thus a collimator located in the second quadrupole can be used to define the momentum bite, 1.2 %. The following quadrupoles (Q2 through Q6) were arranged as field lenses horizontally to give optimum transmission of the accepted momentum bite. In addition, the horizontal optics included two bending magnets (BM1 and BM2). The first is required to avoid a Bevatron building support column. The second bending magnet is used after the third separator system as a clearing field to sweep off-momentum components out of the beam.

The velocity selection was achieved in the vertical plane by deflecting the undesired pions and muons out of the median horizontal plane. The crossed fields of the parallel-plate velocity spectrometers[9] are set for transmission of antiprotons with velocity $\beta^0 = E/H$, which in turn results in the deflection of the lighter kaons, pions, and muons

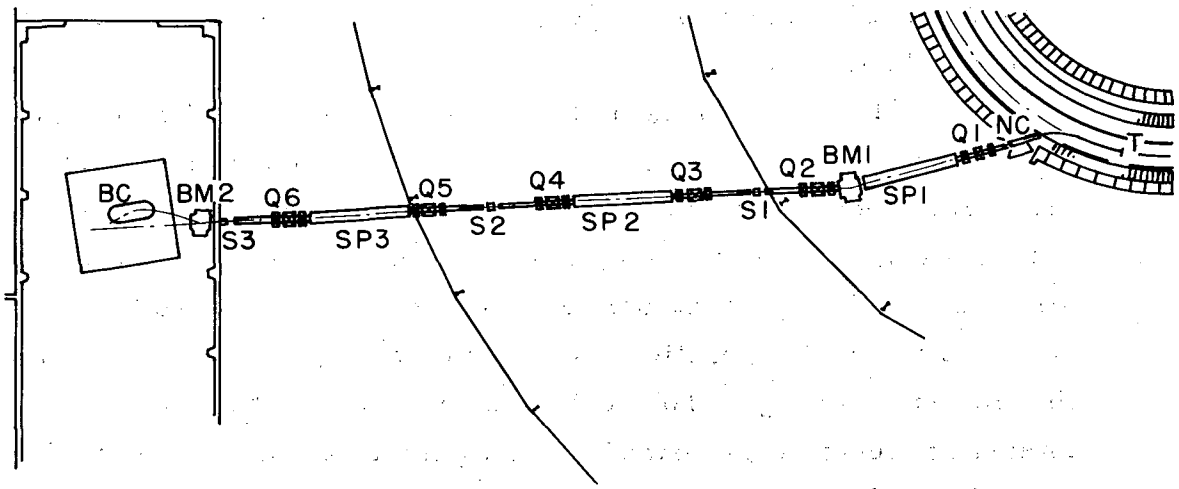


MU-21076

Fig. 1. Beam layout. The antiprotons were produced in the target (T) by the 6.2-Bev proton beam of the Bevatron and were directed over a 200-ft path to the 72-in. liquid hydrogen bubble chamber (BC). The beam channel consisted of a "nose cone" magnetic shield, NC, six triplet 8-in. quadrupoles (Q1 through Q6), two bending magnets (BM1 and BM2), three parallel-plate velocity spectrometers (SP1, SP2, SP3), and three slits (S1, S2, S3).

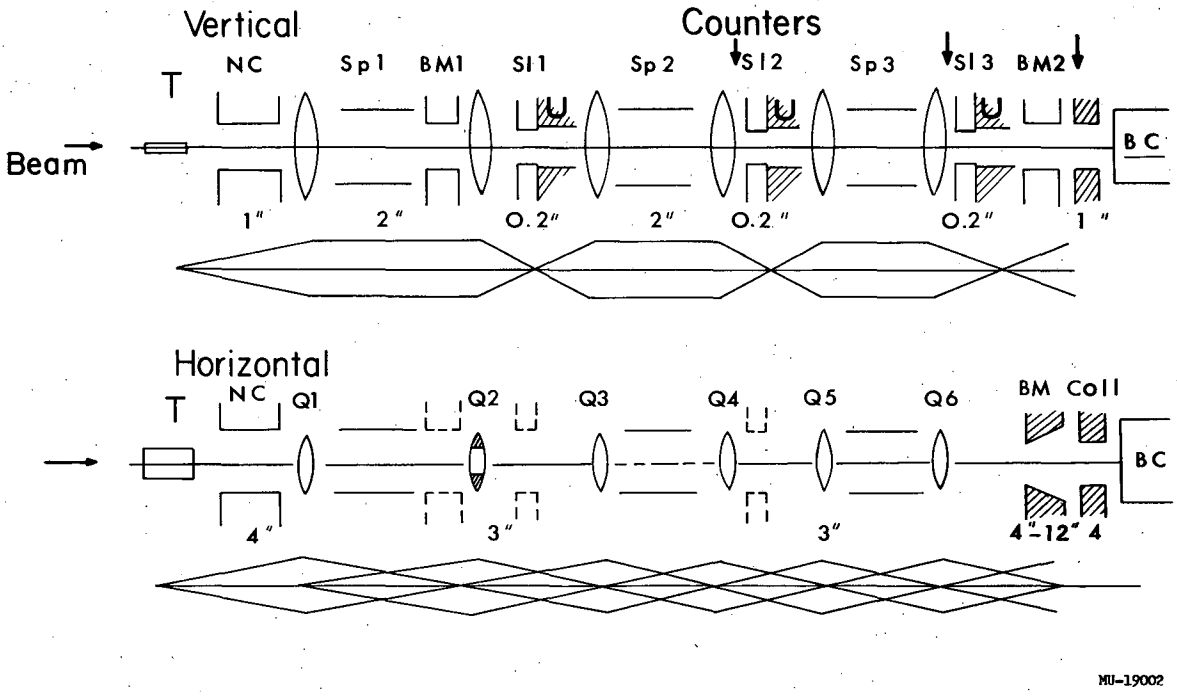


Fig. 2. Schematic diagram of the optics of the 1.61-Bev/c separated beam. Here U is the uranium collimator or absorber; other symbols shown are defined in Fig. 1.

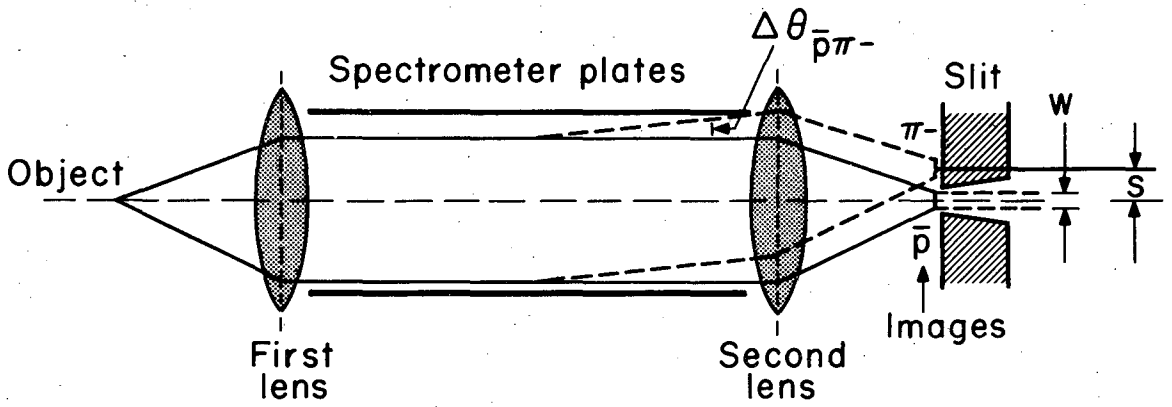


Fig. 3. Optics in the vertical plane for one separator system. The angular separation $\Delta\theta$ is transformed into the spatial separation S. The width W of the image depends on the size of the object, the chromatic and spherical aberrations of the electric and magnetic fields, and the multiple Coulomb scattering in the windows of the vacuum systems. The ratio of W to S determines the effectiveness of the system for the rejection of the undesired particles.

Table III. Summary of beam characteristics.

| | |
|---|---|
| Energy of protons incident on Bevatron target | 6.2 Bev |
| Antiproton beam | |
| Momentum at target | 1.64 Bev/c |
| Momentum at center of bubble chamber | 1.61 Bev/c ($E_{c.m.}$ =2.29 Bev) |
| Momentum bite at bubble chamber | 0.020 Bev/c ($\Delta E_{c.m.}$ =0.007 Bev) |
| Transmission of total system | 0.33 |
| Average $\bar{p}$ flux per picture | 0.8 |
| Target | |
| Material | Aluminum |
| Size: Azimuthal | 5 in. |
| Radial | 1/2 in. |
| Vertical | 1/8 in. |
| Separation | |
| Average operating voltage of the parallel-plate velocity spectrometers | 385 kv |
| Average angular separation | 3.1 mrad |
| Image width W (vertical)at slits | 0.20, 0.18, and 0.40 in. |
| Separation S per stage | 0.50, 0.40, and 0.40 in. |
| W/S | 0.40, 0.45, and 1.0 in. |
| $\pi/\bar{p}$ ratios At target | 20,000/1 |
| At bubble chamber | 0.36/1 |
| Total rejection ratio for pions | $5\times10^4$ |
| Beam composition and total flux | |
| Average beam composition in bubble chamber ($\bar{p}/\pi^-/\mu^-/K^-$) | 1.0/0.36/2.8/0.002 |
| Total number of antiprotons | 46,000 |
| Number of antiproton interactions | 20,900 |

Transformation to $\bar{p}$-p center of mass

$E_{c.m.}$ = 2.290 Bev, $p_{c.m.}$ = 0.658 Bev/c, $\gamma$ = 1.22, $\eta$ = 0.70

out of the median plane by an angle $\Delta\theta = \frac{ev}{cp} \frac{L}{d} \Delta \frac{1}{\beta}$ radians, where p is the momentum of the particle in ev/c, v is the voltage applied to the spectrometer plates, d is the separation of the plates, L is the length of the plates, and the difference in $\frac{1}{\beta}$ for the two velocities in question is defined by $\Delta \frac{1}{\beta} = \frac{1}{\beta} - \frac{1}{\beta_0}$.

At the end of each separation system a magnetic slit backed up by uranium was used to stop the deflected particles. The slit, in turn, was in effect the source of antiprotons for the following part of the system.

The characteristics of the target, the beam, and the optical system are listed in detail in Table III.

## Beam Control

The system is tuned to transmit the intense pion beam, the position of which is determined by measurements with a hodoscope of scintillation counters, and then the magnetic fields of the spectrometers are adjusted to transmit particles with the velocity of the antiprotons.

The magnetic field $H_{\bar{p}}$ required in each system to transmit the antiprotons can be calculated by

$$(H_{\bar{p}} - H_0) = (\beta_\pi/\beta_{\bar{p}})(H_\pi - H_0),$$

where $H_0$ is the magnetic field required for transmitting the pion beam with no voltage applied to the spectrometer plates, $H_\pi$ is the magnetic field with the desired operating voltages, and $\beta_\pi$ and $\beta_{\bar{p}}$ are the velocities of the pions and antiprotons respectively.

After the spectrometers were adjusted to transmit the antiprotons, the hodoscope was moved off the center line of the slit into the rejected pion image. Thereafter minor changes in voltage and current were compensated by adjustments to keep the rejected image centered in the hodoscope. Periodically, the whole adjustment procedure was repeated in order to maintain optimum transmission over the long period of operation of this beam (approximately 2 months).

## III. SELECTION OF EVENTS

The reaction $\bar{p} + p \rightarrow 3\pi^+ + 3\pi^- + n\pi^0$ can be recognized by a negative beam track producing a six-prong event. Figure 4 shows a typical six-prong event. For optimum elimination of the pion background we used only film taken when the spectrometer voltage was higher than 350 kv. After this selection, there were approximately 80 rolls of film. Each roll of film contains approximately 600 frames three stereo views for each frame). To improve the efficiency of the detection and the precision of the measurement of the events, we also exclude from the sample the interactions occurring in the end zones (zones 0 and 9). Some additional events were rejected because of splices of the film, faintness of track, etc. The number of pion interactions is determined by the number of $\delta$ rays on the corresponding incident tracks.[10] Our scanners were instructed to record $\delta$ rays greater than 1 cm in diameter on the scanning tables (these correspond to electrons with momenta greater than 4.14 Mev/c, and cannot be produced by 1.61-Bev/c antiprotons). The expected ratio of recordable $\delta$ rays on interacting pion tracks to the number of pion interactions is 0.155 (based on a pion total cross section of 33 mb and a path length of 69 in.).

The number of antiproton interactions is calculated as the difference between the total number of interactions and the estimated number of pion interactions.

The beam composition is given in Table III above. The numbers of interactions are given in Table IV.

Table IV. Number of interactions in good sample.

| Number of prongs | Total interactions | Pion interactions | Antiproton interactions |
|---|---|---|---|
| 0 | 1604±40 | 358±90 | 1240 |
| 2 | 9692±100 | 1533±220 | 8159 |
| 4 | 4559±70 | 183±50 | 4426 |
| 6 | 715±28 | 0 | 715 |
| 8 | 16±4 | 0 | 16 |
| Total | 16,586±130 | 2,074±270 | 14,556±300 |

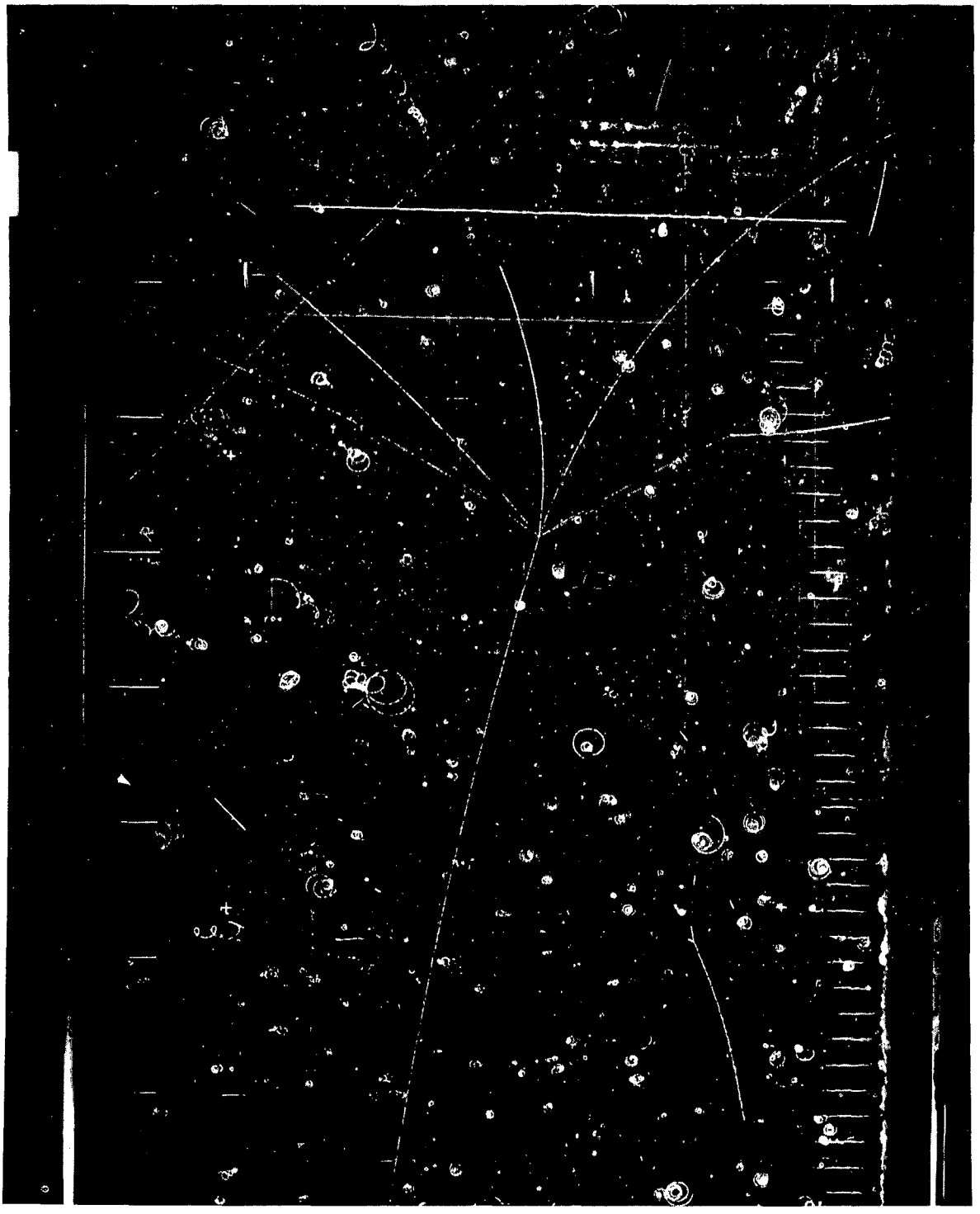

ZN-3092

Fig. 4. A typical 6-prong event.

## IV. MEASUREMENT AND FITTING OF EVENTS

Of the 715 six-prong events 57 were rejected on the scanning table because they showed characteristics of a Dalitz pair, and 63 were rejected because they were unmeasurable. The remaining 595 events constitute an almost pure sample of $\bar{p} + p \rightarrow 3\pi^+ + 3\pi^- + n\pi^0$. Of these events less than 1% are $\pi^- + p \rightarrow p + 3\pi^- + 2\pi^+ + n\pi^0$ (we have seen no $\delta$ rays connected with a six-prong event). Likewise, George Kalbfleisch has shown that less than 1% of these events are annihilations involving kaons;[8] the biggest contamination came from events with four charged pions and a Dalitz pair. But these events can be eliminated after fitting because they show a negative missing energy or an imaginary missing mass (see Appendix 2). All 595 events were measured with the Franckenstein measuring projector for the 72-inch bubble chamber.[11] The track reconstructions were performed with the IBM computer program called "PANG".[12] This program computes the momentum, azimuthal angle, and dip angle for each track.

After track reconstruction, a least-squares fit of the events was performed with the IBM program KICK.[13] We tried to fit the events to the reactions

$$\bar{p} + p \rightarrow 3\pi^+ + 3\pi^-, \qquad (1)$$

$$\bar{p} + p \rightarrow 3\pi^+ + 3\pi^- + \pi^0. \qquad (2)$$

For each fit, a $\chi^2$ function is computed which measures the goodness of the fit.

Normally KICK can handle only seven particles and can at most fit Reaction (1). We have to fit Reaction (2) by considering the antiproton plus proton as a body which decays into seven pions. (Before fitting the decay of a $\bar{p}p$ particle of zero momentum and zero energy into seven pions, we add the approperiate momentum and energy to the particle: momentum = momentum of $\bar{p}$; energy = energy of $\bar{p}$ + mass of proton).

This way we must ignore the uncertainty in the momentum and angle of the $\bar{p}$. But by making use of the known characteristics of the

beam, we reduce the uncertainty in the momentum of $\bar{p}$ to less than 2%, and because the incident track is generally long, the measured momentum error is often less than 0.5%; also, the errors on the angles of the beam are small. To make a check we fit the hypothesis (1) in the normal way and in the new way ($\bar{p}p$ body decaying into six pions). We find that all the fitted values are about the same and that the ratio of the average of the new $\chi^2$ to the average of the old $\chi^2$ is about 1.6, which agrees more or less with a theoretical estimate of 18/15.

An event is considered fitted to Reaction (1) when it has $\chi^2 \leq 30.0$ for this hypothesis. It is considered fitted to Reaction (2) when it has $\chi^2 \leq 5.1$ for this hypothesis and $\chi^2 > 30.0$ for Hypothesis (1).

For Reaction (2) (one constraint) a $\chi^2$ of 5.1 corresponds to a confidence level of 3%. For Reaction (1) (four constraints), the same confidence level would correspond to a $\chi^2$ of about 10, but—as we will see later--our experimental distribution of this reaction seems to be three times that expected; this gives us 30 as a reasonable cutoff value.

When an event does not fit either Reaction (1) or Reaction (2) and has a missing mass $\geq$270 Mev (minus 1 standard deviation) it may have two or more neutral pions missing. Such events were put in a third category called "8π events."

Every event that was rejected by PANG or by KICK or that had a measurement error greater than 50% on the momentum of any track was examined on the scanning table and sent back to be remeasured.

Of the 595 events measured,

153 fitted Hypothesis (1); let us call them "6π events";

239 fitted Hypothesis (2), and were called "7π events";

139 were classified as "8π events";

28 were found to have a negative energy or imaginary missing mass and could be attributed to a Dalitz pair associated with four-prong events (see Appendix 2);

36 remaining were due to bad measurements.

The total number of Dalitz pairs associated with four prongs is thus 57 + 28 = 85; this agrees very well with the prediction (84)

of a Lorentz-invariant statistical model using an interaction volume of $5(4\pi/3)(\hbar/m_\pi c)^3$, which gives a good charged-pion multiplicity at various energies.[14]

It is interesting to see that the $\chi^2$ distribution for Hypothesis (2) (Fig. 5), which has only one constraint, can be compared somewhat to the theoretical curve, whereas the one for Hypothesis (1) (Fig. 6), which has four constraints, can be compared to the theoretical curve only if we multiply the scale of the latter by a factor of 3. (This could be due to underestimated uncertainties in the measured variable) (see Appendix 3).

On the other hand, the missing-mass distribution of both the $6\pi$ events (Fig. 7) and the $7\pi$ events (Fig. 8) look very good and very symmetrical. We believe that about 85% of the 139 $8\pi$ events actually do have two missing pions, because the missing-mass distribution of these events follows, within statistics, the effective mass distribution of two charged pions coming from the same event (Fig. 9).

An examination of the missing-mass distribution as well as the $\chi^2$ distribution convinces us that the $7\pi$ events contain a contamination of less than 17% of the "eight-body" annihilation and about 3% of the "six-body" annihilations. On the other hand, roughly 10% of the true seven-body events have been excluded from the sample and are grouped with the $6\pi$ and $8\pi$ events.

Further processing of the events was done by an IBM 709 program called EXAMIN.[15] The EXAMIN program consists basically of various Fortran language subroutines which calculate the various quantities of physical interest desired by the experimenter. For example, for an event it calculates the momentum and the c.m. angle (relative to beam) of each particle, and the cosines of the angle between all pairs of final particles in the $\bar{p}$-p center-of-mass system. It also calculates the effective mass of 2, 3, 4, or 5 pions with all possible combinations of charges.

The effective mass is given by the equation

$$M_n = \left[ \left( \sum_1^n E_i \right)^2 - \left| \sum_1^n \vec{p}_i \right|^2 \right]^{1/2} ,$$

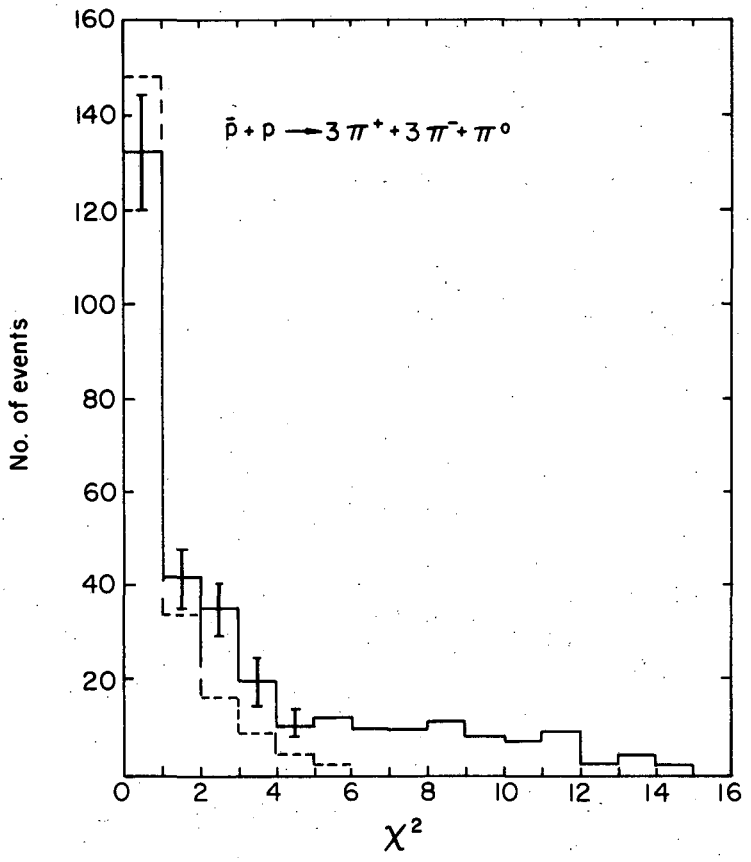


Fig. 5. Comparison of $\chi^2$ distribution for $\bar{p} + p \rightarrow 3\pi^+ + 3\pi^- + \pi^0$ events (one constraint), ——— , with theoretical $\chi^2$ distribution, ---- .

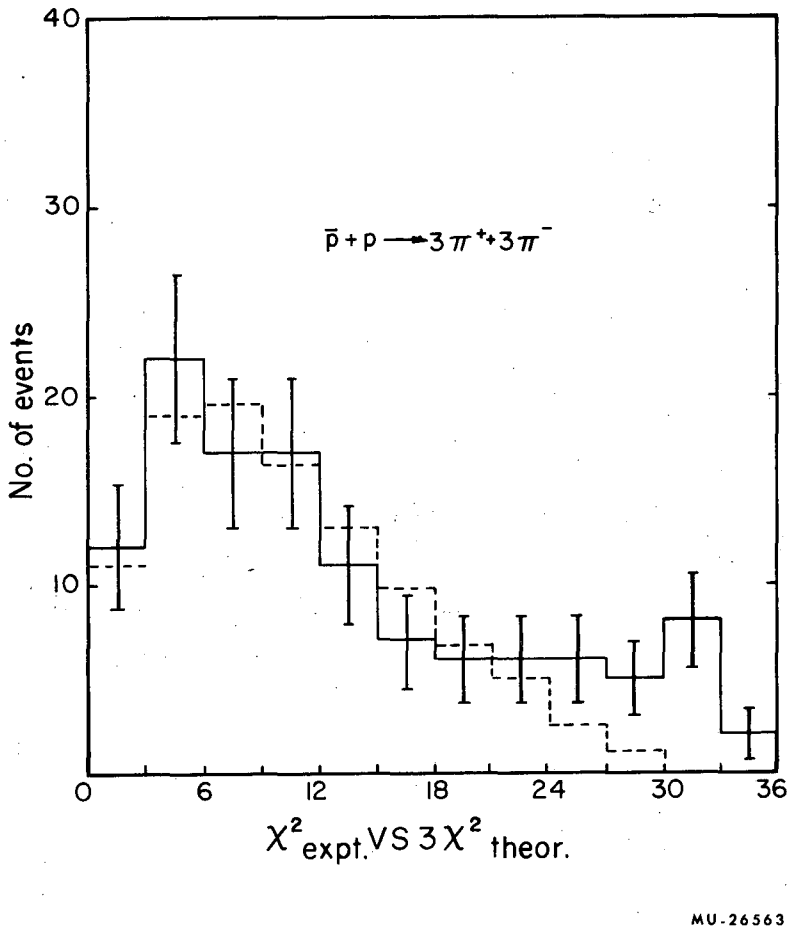


Fig. 6. Comparison of $\chi^2$ distribution for $\bar{p}+p \rightarrow 3\pi^+ + 3\pi^-$ events (four constraints), _____, with theoretical $\chi^2$ distribution, - - - . Scale factor of 3 for the latter.

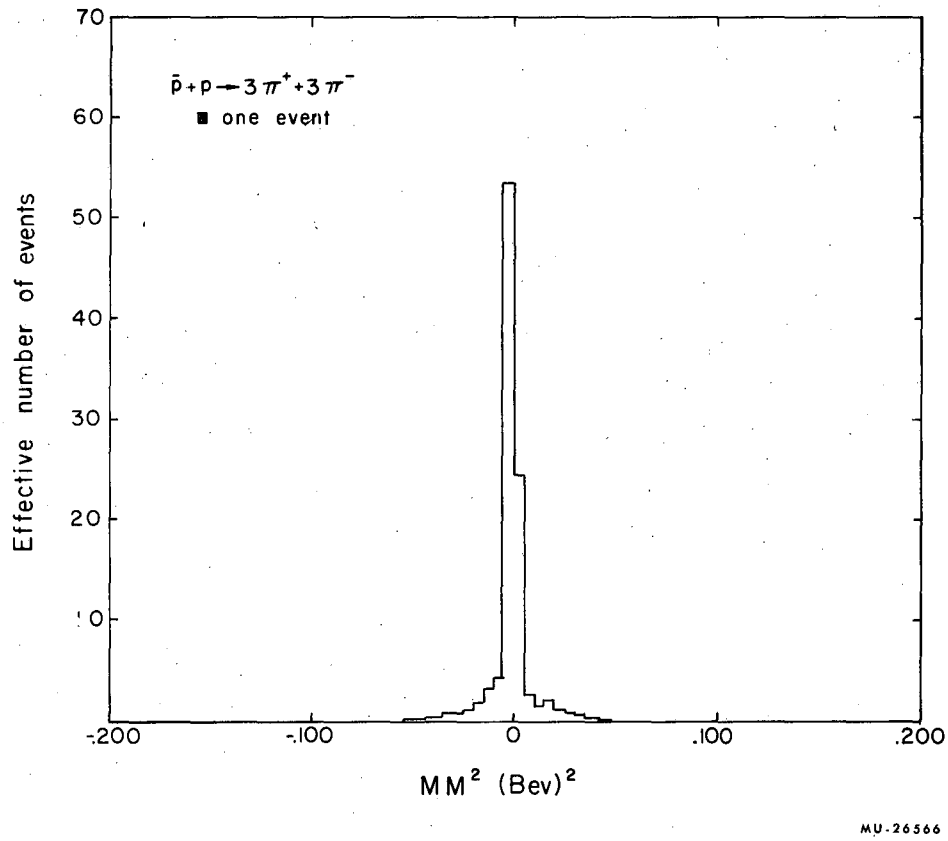


Fig. 7. Distribution of the square of the missing mass ($MM^2$) for "6π" events.

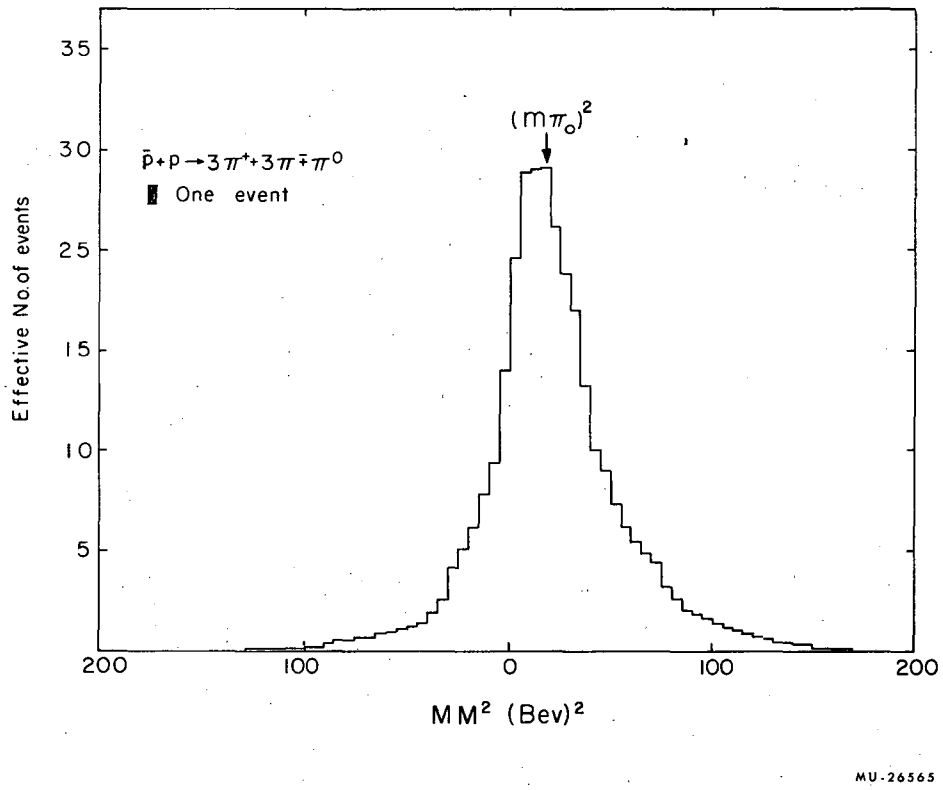


Fig. 8. Distribution of the square of the missing mass for "7π" events.

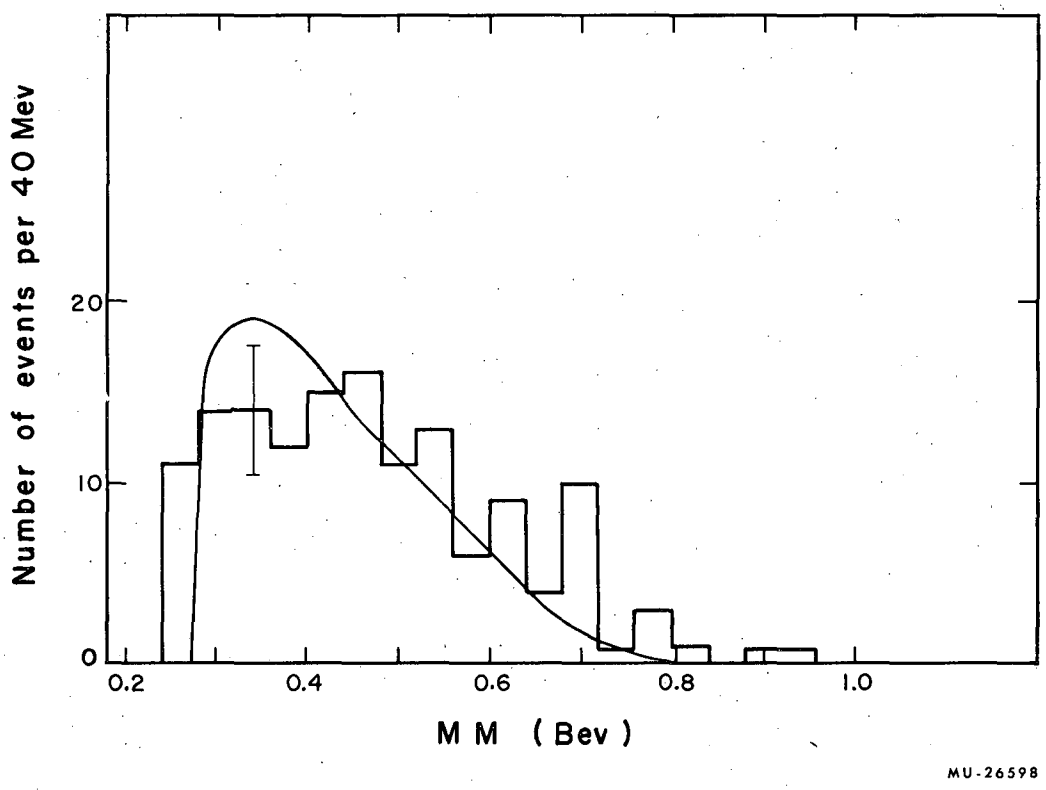


Fig. 9. Distribution of the missing mass of the "8π" event. The solid curve is drawn from the distribution of the effective mass of two charged pions from the same events.

where n indicates the number of pions included in the effective mass, and $E_i$ and $\vec{p}_i$ are the energy and momentum respectively of the ith particle. We calculated for each value of $M_n$ an uncertainty $\delta M_n$ by using the variance-covariance matrix of the fitted-track variables, which is evaluated by KICK.

All the important quantities are stored in one magnetic tape called a summary tape.

Many small Fortran 709 IBM programs then use this tape to pick out the right quantities, make comparisons, or make histograms or ideograms, or even make further calculations if necessary.

# V. PRESENTATION AND DISCUSSION OF RESULTS

## A. Cross Section, Momentum Distribution, and Angular Distribution

### Cross section

To determine the cross sections of $6\pi$, $7\pi$, and $8\pi$ events, we make use of the known antiproton-proton total cross section at 1.61 Bev/c,[16]

$$\sigma_{total} = 96 \pm 3 \text{mb}.$$

We estimate about 3 mb for the cross section of elastic scattering at very small angles, where the recoil proton track is too short to be detected by our scanners. Thus a cross section of $93 \pm 3$ mb corresponds to $14{,}556 \pm 300$ interactions in our sample, of which 715 - 85 = 630 are six-prong events. Because of rejection of events due to difficulty of measurement, we have to apply a correction factor of $630/(153+239+139) = 1.19$ to the number of $6\pi$, $7\pi$, and $8\pi$ events.

To estimate the scanning efficiency for six-prong events, we make an independent second scan of about one-half of our sample. By comparing the results of this scan with the one of the first scan we find a remarkable efficiency of 99% for each separate scan.

The cross sections are then found to be

$$\sigma(\bar{p} + p \rightarrow 3\pi^+ + 3\pi^-) = 1.16 \pm .1 \text{ mb},$$

$$\sigma(\bar{p} + p \rightarrow 3\pi^+ + 3\pi^- + \pi^0) = 1.80 \pm .25 \text{ mb},$$

$$\sigma(\bar{p} + p \rightarrow 3\pi^+ + 3\pi^- + 2\pi^0) = 1.05 \pm .25 \text{ mb}.$$

Table V shows the cross sections of antiproton-proton processes at 1.61 Bev/c.

### Momentum distribution

Figure 10 shows the momentum distribution in the $\bar{p}$-p center-of-mass system, respectively for $\pi^+$, $\pi^-$, and both $\pi^+$ and $\pi^-$ for the $6\pi$ events. The curves represent the Lorentz-invariant phase-space calculations. We observe that $\pi^+$ - and $\pi^-$ meson distributions are alike, as predicted by CP invariance,[19] and that both of them agree very well with the phase-space calculation.

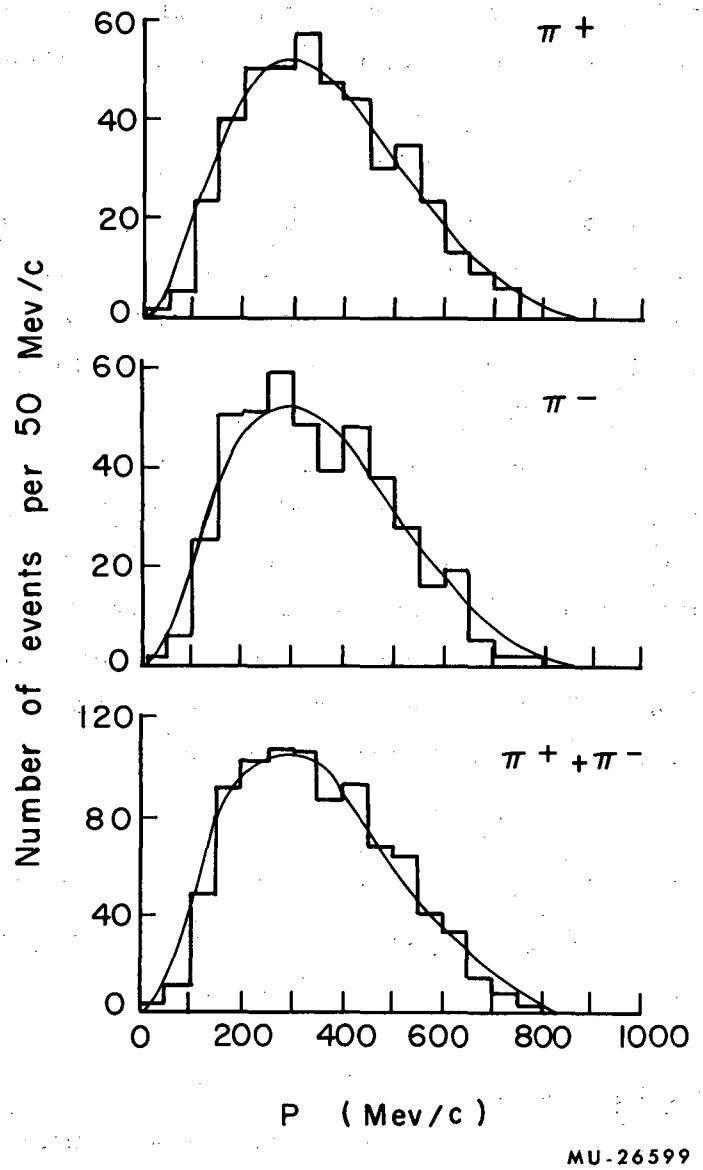


Fig. 10. Center-of-mass momentum distribution for pions of "6π" events, $\bar{p} + p \rightarrow 3\pi^+ + 3\pi^-$. Top, $\pi^+$; center, $\pi^-$; bottom, $\pi^+$ and $\pi^-$. The solid curves represent the Lorentz-invariant phase-space calculation. (153 events.)

Table V. Cross sections of diverse processes of $\bar{p}$-p interactions at 1.61 Bev/c ($E_{c.m.}$ = 2.290 Bev).

(The total cross section is 96±π mb from Ref. 3.)

| Process | Reference | Cross section (mb) |
|---|---|---|
| Elastic | | |
| $\bar{p}+p \rightarrow \bar{p}+p$ | 16 | 33±3. |
| Charge-exchange | | |
| $\bar{p}+p \rightarrow \bar{n}+n$ (and) $\bar{n}+n+\pi^0$ | 16 | 7.8±.55 |
| Inelastic | | |
| $\bar{p}+p \rightarrow \bar{p}+p+\pi^0$ | 14 | 1.6±.30 |
| $\rightarrow \bar{n}+p+\pi^-$ | 14 | 0.96±.22 |
| $\rightarrow \bar{p}+n+\pi^+$ | 14 | 1.15±.30 |
| Hyperon-antihyperon | | |
| $\bar{p}+p \rightarrow \Lambda+\bar{\Lambda}$ | 8 | 0.057±.018 |
| Annihilation involving | | |
| K Mesons and π mesons | | |
| $\bar{p}+p \rightarrow K^0+\bar{K}$ | 14 | 0.055±.018 |
| $\rightarrow K^+ + K^-$ | 14 | ≤ .050 |
| $\bar{p}+p \rightarrow K+\bar{K}+\pi$ | 8 | 0.74±.16 |
| $\rightarrow K+\bar{K}+2\pi$ | 8 | 1.95±.26 |
| $\rightarrow K+\bar{K}+3\pi$ | 8 | 2.2±.26 |
| $\rightarrow K+\bar{K}+4\pi$ | 8 | 0.37±.011 |
| $\rightarrow K+\bar{K}+5\pi$ | 8 | $0^{+.02}_{-0}$ |
| Annihilation involving π Mesons | | |
| $\bar{p}+p \rightarrow n\pi^0$, for $n \geq 2$ | 14 | $0.3^{+.4}_{-.3}$ |
| $\bar{p}+p \rightarrow \pi^+ + \pi^-$ | 14 | 0.1±.025 |
| $\rightarrow \pi^+ + \pi^- + \pi^0$ | 14 | 2.5±1.5 |
| $\rightarrow \pi^+ + \pi^- + n\pi^0$ for $n \geq 2$ | 14 | 14.1±3. |
| $\rightarrow 2\pi^+ + 2\pi^-$ | 17 | 1.4±.3 |

Table V. (cont.)

| Process | Reference | Cross section (mb) |
|---|---|---|
| Annihilation involving $\pi$ Mesons | | |
| $\bar{p} + p \rightarrow 2\pi^+ + 2\pi^- + \pi^0$ | 17 | 10.4±1.0 |
| $\rightarrow 2\pi^+ + 2\pi^- + n\pi^0$, for $n \geq 2$ | 17 | 12.0±1.5 |
| $\rightarrow 3\pi^+ + 3\pi^-$ | | 1.2±.1 |
| $\rightarrow 3\pi^+ + 3\pi + \pi^0$ | | 1.8±.25 |
| $\rightarrow 3\pi^+ + 3\pi + 2\pi^0$ | | 1.05±.25 |
| $\rightarrow 4\pi^+ + 4\pi^-$ | 18 | 0.025±.01 |
| $\rightarrow 4\pi^+ + 4\pi^- + \pi^0$ | 18 | 0.006±.006 |

Figures 11 and 12 show the momentum distributions in the $\bar{p}$-p center-of-mass system for the charged pions only in the 7 $\pi$ events and in the 8 $\pi$ events. Here we do not yet have the phase-space calculation, but we observed that the $\pi^+$-meson distribution agrees with the $\pi^-$-meson distribution, and neither shows any significant peaks.

Figure 13 shows the c.m. momentum distribution of the neutral $\pi$ of the 7 $\pi$ events. This distribution agrees very well with the distribution of charged pions from the same event (Fig. 10). If a real 6 $\pi$ event were mistaken as a 7 $\pi$ event, the fake $\pi^0$ would have a small momentum in the laboratory system; in the $\bar{p}$-p c.m. system its momentum would be about 100 Mev/c or less. As shown in Fig. 13, we have 14 events with $p_{\pi^0} \leq 100$ Mev/c. From the c.m. momentum distribution of charged pions of 7 $\pi$ events (Fig. 11) we can estimate nine true 7 $\pi$ events (52/6) with $p_{\pi^0} \leq 100$ Mev/c. This gives us an estimation of about 14 - 9 = 5 real 6 $\pi$ events that are mistaken as 7 $\pi$ events.

Angular distribution

The c.m. angular distributions for $\pi^+$ and $\pi^-$ mesons of 6 $\pi$, 7 $\pi$, and 8 $\pi$ events are plotted respectively in Figs. 14, 15, and 16. As espected on the basis of C and CP,[19] the distributions of $\pi^+$ appear to be equal, within statistics, to the reflections of the angular distribution of the $\pi^-$'s. For the three types of events, we have reflected the $\pi^-$ distribution about $\cos\theta = 0$, added it to the $\pi^+$ distribution, and plotted them in the bottom histograms in Fig. 14, 15, and 16. All these distributions look very symmetrical and become more and more isotropic as the number of pions increases. These results are in contrast with the asymmetry found by Maglić, Kalbfleisch, and Stevenson in the angular distribution of $\pi^\pm$ mesons coming from the reaction $\bar{p} + p \rightarrow 2\pi^+ + 2\pi^- + n\pi^0$ at the same antiproton energy.[20] One explanation could come from the Koba and Takeda theory,[21] which assumes that about two annihilation pions are emitted from the antiproton and proton clouds. Those pions would be responsible for the asymmetry in the

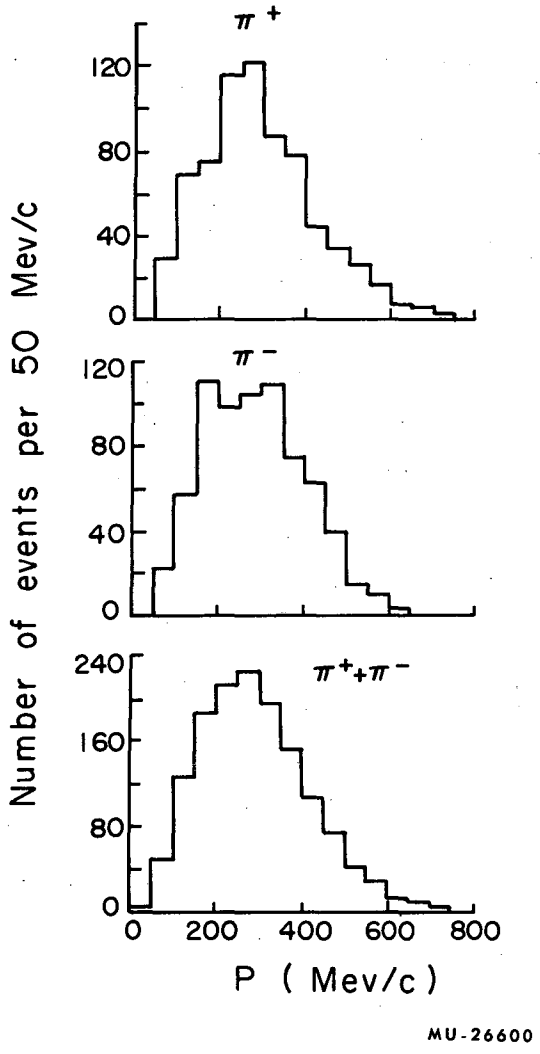


Fig. 11. Momentum distribution (c.m.) for charged pions of $7\pi$ events, $\bar{p} + p \rightarrow 3\pi^+ + 3\pi^- + \pi^0$.
Top, $\pi^+$; center, $\pi^-$; bottom, $\pi^+$ and $\pi^-$. (239 events.)

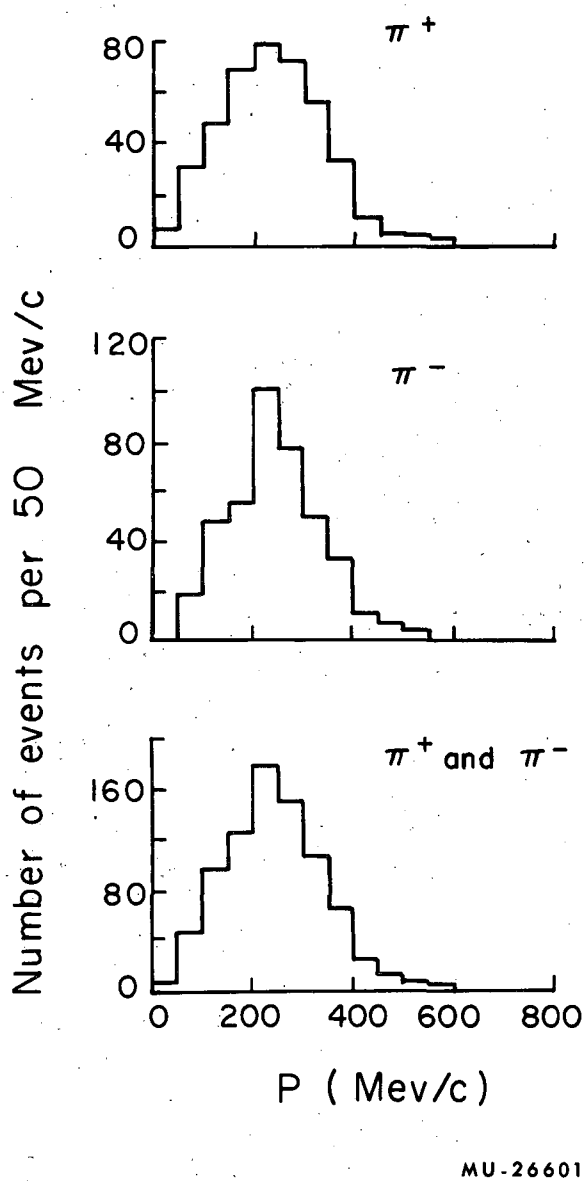


Fig. 12. Momentum distribution (c.m.) for charged pions of 8π events, $\bar{p} + p \rightarrow 3\pi^+ + 3\pi^- + 2\pi^0$. Top, $\pi^+$; center, $\pi^-$; bottom, $\pi^+$ and $\pi^-$. (139 events.)

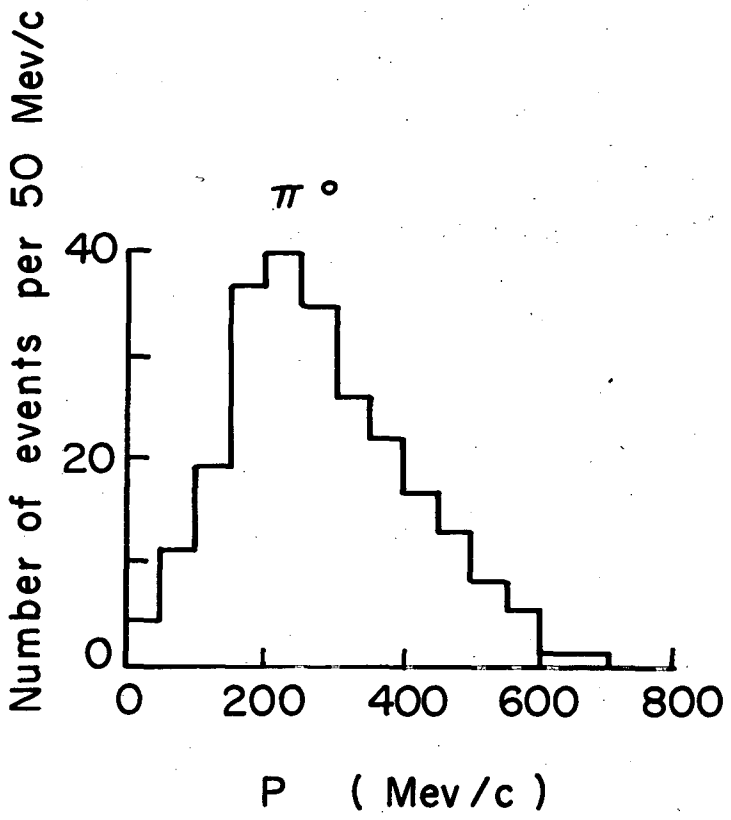


Fig. 13. Momentum distribution (c.m.) for neutral pions of 7π events.

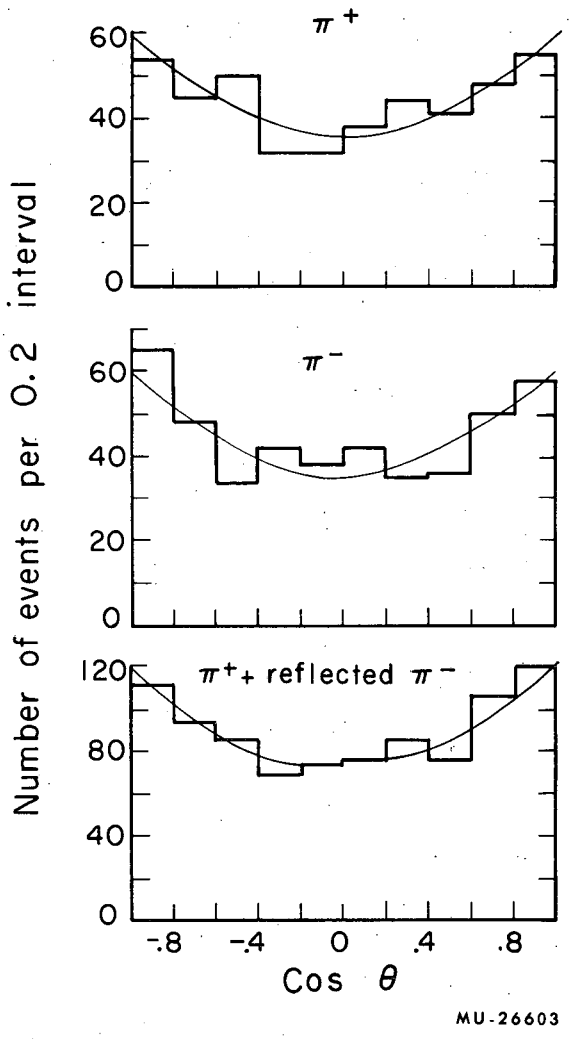


Fig. 14. Distribution of cosine of c.m. production angle for individual charged pions of 6π events. Top, $\pi^+$; center, $\pi^-$; bottom, $\pi^+$ and reflected $\pi^-$. (153 events.)

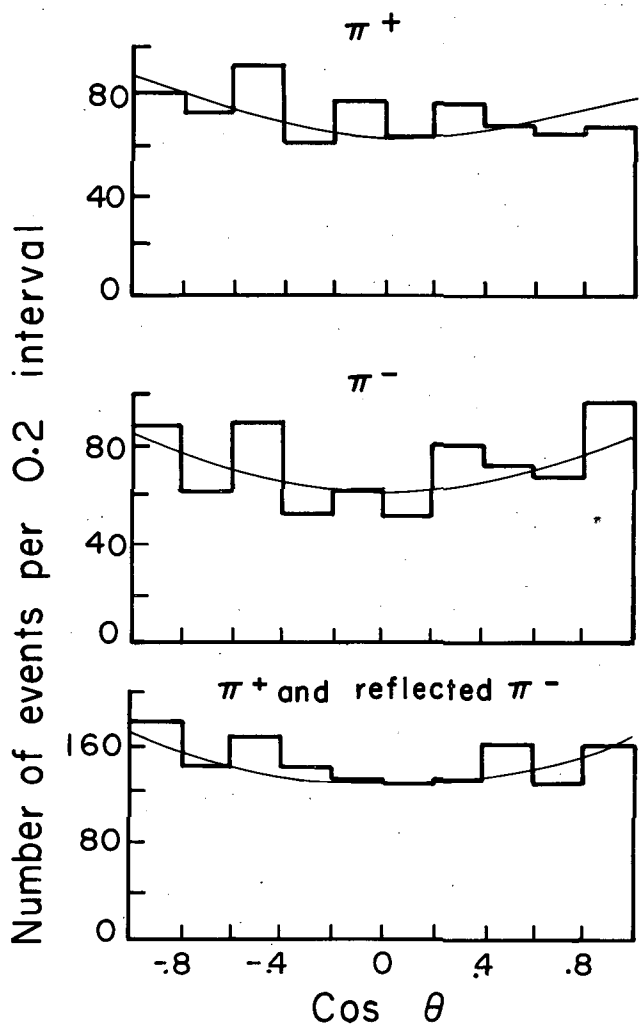


Fig. 15. Distribution of cosine of c.m. production angle for individual charged pions of 7π events.
Top, $\pi^+$; center, $\pi^-$; bottom, $\pi^+$ and reflected $\pi^-$.
(239 events.)

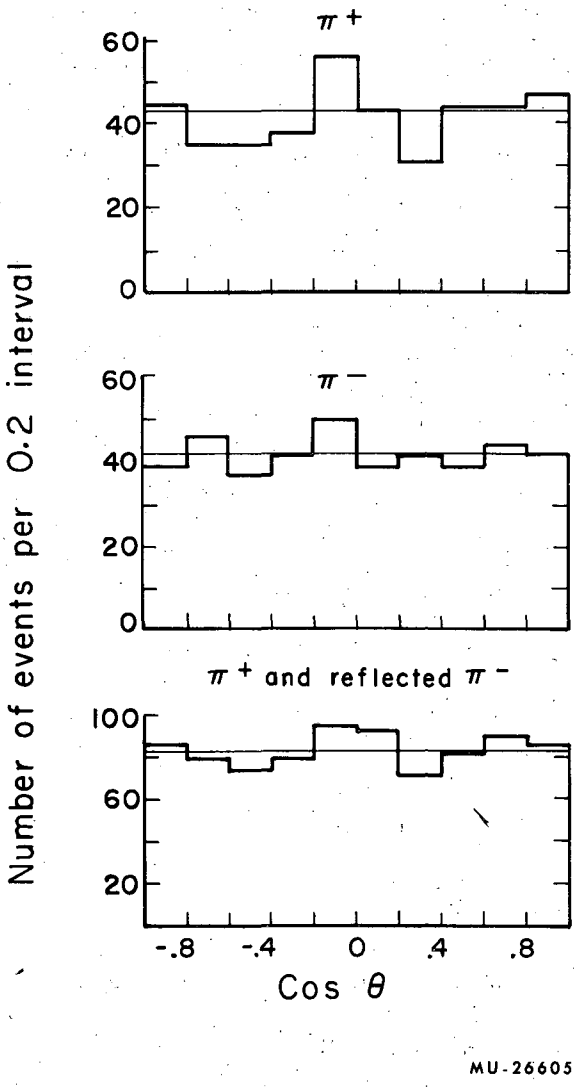


Fig. 16. Distribution of cosine of c.m. production angle for individual charged pions of 8π events.
Top, $\pi^+$; center, $\pi^-$; bottom, $\pi^+$ and reflected $\pi^-$.
(139 events.)

angular distribution. In the $6\pi$, $7\pi$, and $8\pi$ events, the ratio of "cloud" pions over "core" pions is smaller than in the $4\pi$ and $5\pi$ events, ($\bar{p} + p \to 2\pi^+ + 2\pi^-$ and $\bar{p} + p \to 2\pi^+ + 2\pi^- + \pi^0$), and the asymmetry can be masked. It is true also that the numbers of $6\pi$, $7\pi$, and $8\pi$ events are much smaller than the numbers of $4\pi$ and $5\pi$ events (see Table V) so that we cannot observe a small asymmetry.

Figure 17 (a) shows the angular distribution of $\pi^0$ from the $7\pi$ events. CP predicts this distribution to be symmetrical,[19] but our results seem to show a small forward-backward asymmetry and can be fitted to a $(1 + a \cos\theta)$ distribution with $a = 0.26 \pm .11$. Although it is only 2.3 standard deviations from $a = 0$, we have looked at all possible biases:

(a) It is possible that some real $7\pi$ events with backward $\pi^0$ have been misclassified as $6\pi$ events.

(b) Another bias can come from the real $8\pi$ ($\bar{p} + p \to 3\pi^+ + 3\pi^- + 2\pi^0$) background in our $7\pi$ events ($\bar{p} + p \to 3\pi^+ + 3\pi^- + \pi^0$). Let us use the name "dipi" for the real $2\pi^0$ system and "fake $\pi^0$" for that calculated when it is fitted to a $7\pi$ hypothesis.

In the lab system we have $\vec{p}_{(\text{fake}\,\pi^0)} \approx \vec{p}_{(\text{dipi})} \equiv \vec{p}$, but $E_{(\text{fake})}$ tends to be smaller than $E_{\text{dipi}}$. When the dipi is transformed to the $\bar{p}$-p c.m. system its momentum becomes

$$\begin{cases} p'_{||} = \gamma p_{||} - \eta E_{\text{dipi}}, \\ p'_{\perp} = p_{\perp} \end{cases}.$$

The c.m. momentum of the "fake $\pi^0$" would be

$$\begin{cases} p'_{||} = \gamma p_{||} - \eta E_{\text{fake}\,\pi^0} \\ p'_{\perp} = p_{\perp} \end{cases}.$$

Since $E_{\text{fake}\,\pi^0} < E_{\text{dipi}}$, this makes the component in the $\bar{p}$ direction of the "fake $\pi^0$" too big in the $\bar{p}$-p c.m. system, and therefore produces a fake forward peak.

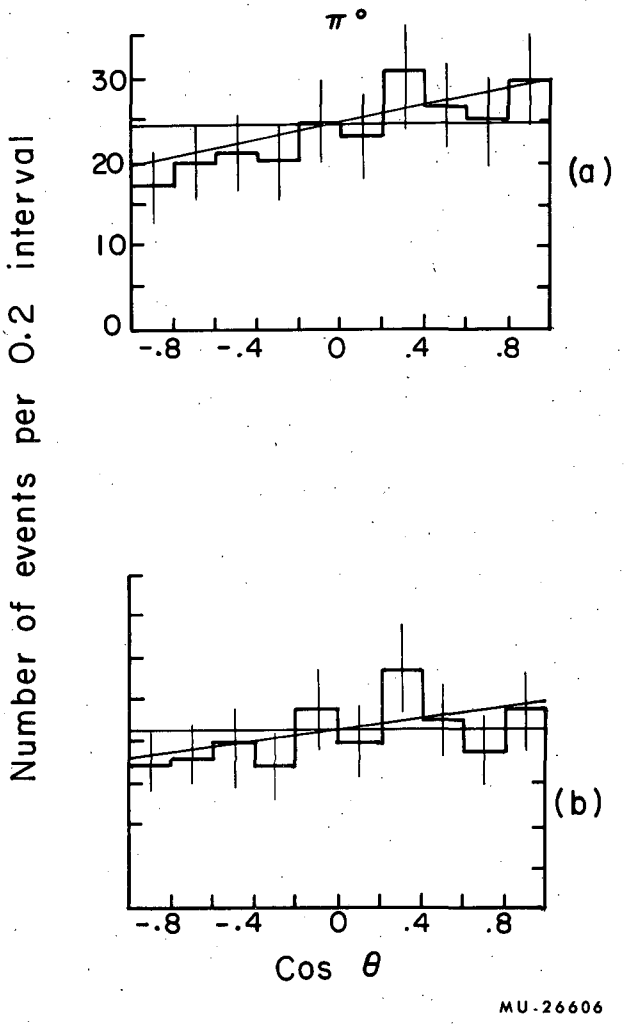


Fig. 17. c.m. angular distribution for neutral pions of 7π events (a) for 239 7π events, (b) same as (a) except that 28 ambiguous events have been excluded.

To check the first bias hypothesis we plot the $\pi^0$ angular distribution of those 15 events which were ambiguous between "6 $\pi$ -7 $\pi$" (15 events with $\chi^2 \leq 30.0$ for the 6 $\pi$ hypothesis and $\chi^2 \leq 5.1$ for the 7 $\pi$ hypotheses). This angular distribution is isotropic and cannot produce the asymmetry observed.

To check the second bias hypothesis we replot in Fig. 17(b) the angular distribution of the 211 7 $\pi$ events excluding the 28 7 $\pi$ - 8 $\pi$ ambiguous events (events with $\chi^2 \leq 5.1$ for the 7 $\pi$ hypothesis but with a missing mass $\geq$270 Mev). This more carefully selected 7 $\pi$ distribution is much less asymmetrical and can be considered as isotropic within statistics. (A best fit gives $1 + (0.15 \pm .12) \cos\theta$.) We conclude that the small forward-backward asymmetry in the angular distribution of $\pi^0$ was due to the 8 $\pi$ background in the 7 $\pi$ events (17%). A $\pi^0$ angular distribution of real 7 $\pi$ events would be isotropic, in agreement with CP prediction. We have also made sure that the association of the "7 $\pi$-8 $\pi$" ambiguous events with either the 7 $\pi$ or the 8 $\pi$ events does not change our other results appreciably.

## B. Effective Mass Distribution of Three Pions

### Existence of the I = 0 Three-Pion Resonance

For each event we have evaluated the three-pion effective mass

$$M_3 = [(E_1 + E_1 + E_3)^2 - (\vec{P}_1 + \vec{P}_2 + \vec{P}_3)^2]^{1/2}$$

The 6 $\pi$ and the 8 $\pi$ events can yield $M_3$ combinations with charge $|Q| = 1$ (that is $\pi^\pm \pi^\pm \pi^\mp$) and $|Q| = 3$ (that is $\pi^\pm \pi^\pm \pi^\pm$). In the 8 $\pi$ events we could also form another combination of $M_3$ with $|Q| = 1$ ($\pi^\pm \pi^0 \pi^0$). The $M_3$ distributions for these triplets do not show any significant peak. These data, however, are less useful than for 7 $\pi$ events for which we can form combinations with $|Q| = 0, 1, 2$ and be able to make comparisons between their distributions.

Each 7 $\pi$ event can yield 33 triplets corresponding to the charge states

| | | |
|---|---|---|
| $Q = 0$ | $\pi^+ \pi^- \pi^0$ | (9 combinations) |
| $\|Q\| = 1$ | $\pi^\pm \pi^\pm \pi^\mp$ | (18 combinations) |
| $\|Q\| = 2$ | $\pi^\pm \pi^\pm \pi^0$ | (6 combinations) |

We calculated for each value of $M_3$ an uncertainty $\delta M_3$ by using the variance-covariance matrix of the fitted track variables, which is evaluated by KICK. The $M_3$ resolution[22] is $\Gamma_{resol}/2 = 9.0$ Mev. However, because of systematic errors known to exist in our track reconstruction, our estimate of $\Gamma_{resol}/2$ probably should be increased by $\sqrt{3}$ to $\Gamma_{resol}/2 = 16$ Mev. (See Appendix 3.).

Figure 18 is a histogram of the $M_3$ distribution for the 239 $7\pi$ events. The distributions (a) and (b) are for the charge combinations $|Q| = 1$ and 2 respectively. To show the difference between the neutral $M_3$ distribution and that for $|Q| \geq 1$, we have replotted at the bottom of Fig. 18 both the neutral distribution and 9/24 of the sum of the $|Q| = 1$ and $|Q| = 2$ distributions. This latter distribution we use as an estimate of the background. The neutral distribution, (c), shows a peak at 780 Mev that contains 79 pion triplets above the background of 238. Figure 19 is a histogram of the neutral distribution around the 780-Mev region.

The peak at 780 Mev can be interpreted as a resonance of isotopic spin $I = 0$, with a half width $\Gamma$ of about 15 Mev. The isotopic spin, of about 15 Mev. The isotopic spin, the energy, and the half width of this resonance agree very well with the $\omega$ meson found by Maglić et al., who analyzed the four-prong annihilations in the same experiment.[23] We must also conclude, as they did, that the half width of the experimental peak is so close to our resolution that the true width of the peak is less than 15 Mev and could be zero.

Of the 239 $7\pi$ events, $79 \pm 18$ (or $33 \pm 8\%$) of these proceed via the reaction $\bar{p} + p \rightarrow \omega + 2\pi^+ + 2\pi^-$, $(\omega \rightarrow \pi^+ \pi^- \pi^0)$, for which the cross section is $0.6 \pm .15$ mb. It is interesting to compare this yield with the $130 \pm 20$ events (or $12 \pm 3\%$) of the $5\pi$ events ($\bar{p} + p \rightarrow 2\pi^+ + 2\pi^- + \pi^0$, studied by Maglić et al.[23]) that proceed via the reaction $\bar{p} + p \rightarrow \omega + \pi^+ + \pi^-$.

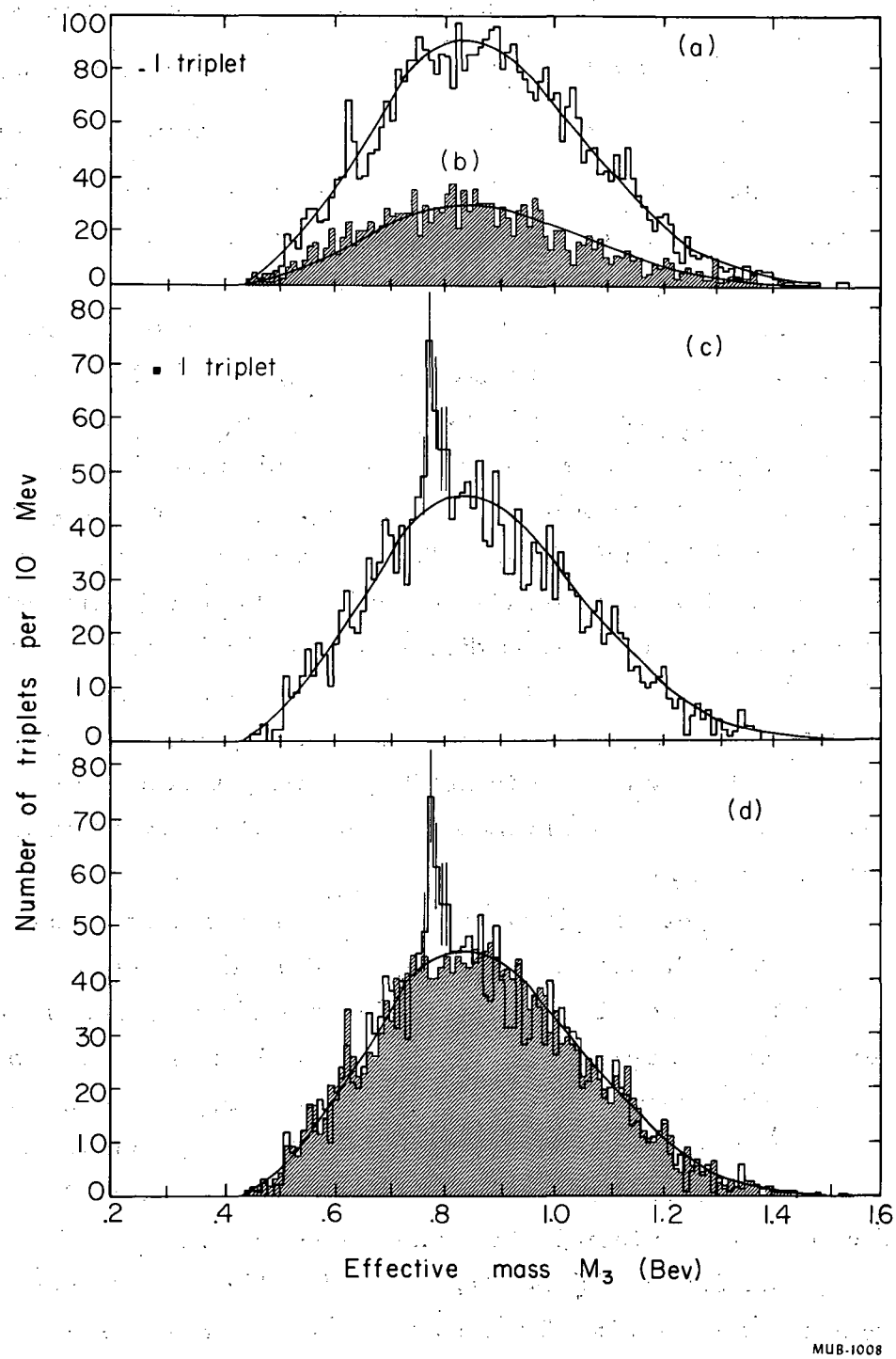


Fig. 18. Histograms of the distributions of the effective masses ($M_3$) of pion triplets for the 7π events, (a) for the distribution for the triplets with $|Q|=1$ (239×18 triplets); (b) with $|Q|=2$ (239×6 triplets); (c), with $Q=0$ (139×9 triplets). In (d) the combined distributions of (a) and (b) (shaded area) are compared with the (c) distribution. The same smooth curve has been drawn on (a), (b), and (c).

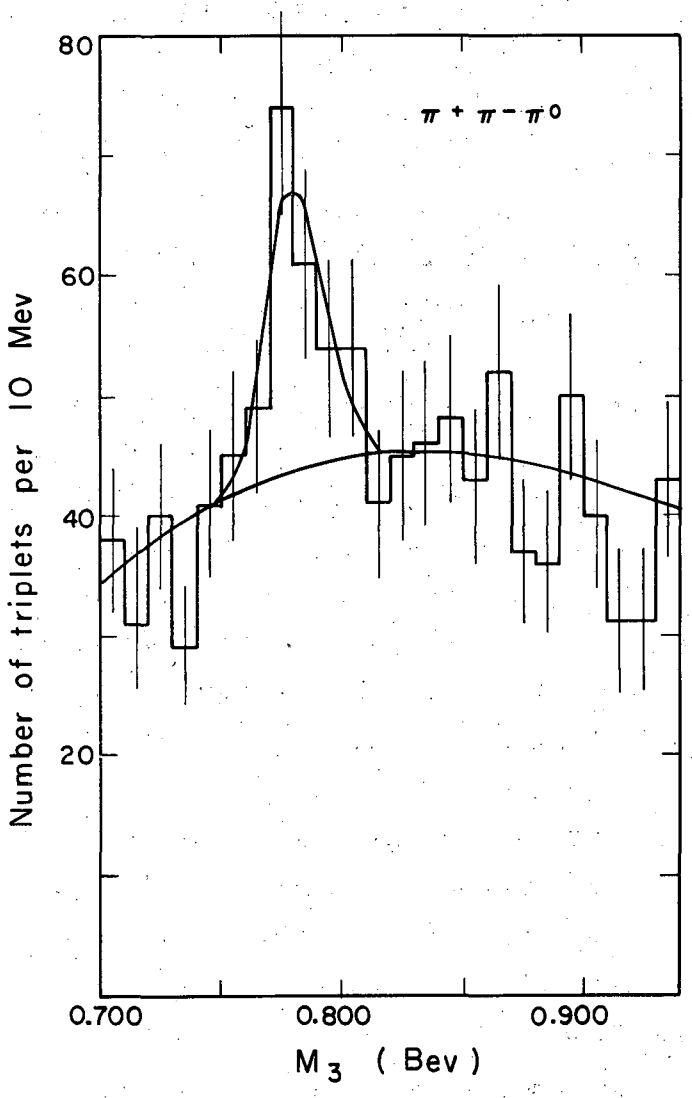


Fig. 19. Histograms of the distribution of neutral $M_3$ for $7\pi$ events, around the 780-Mev region. The resonance curve contains 79 $\omega$ mesons.

Spin and Parity of the ω Meson

To determine the spin and parity of this resonance (or unstable particle) we use the Dalitz plot.[24] We use events of the center of the peak (760 to 800 Mev) and events in a control region (822 to 878 Mev) of the same charge state. About 27% of the triplets in the peak region belong to the resonance. Figures 20 and 21 show the Dalitz plot of the peak-region events and the control-region events, respectively. Unit area on a Dalitz plot is proportional to the corresponding Lorentz-invariant phase space, so that the density of plotted points is proportional to the square of the matrix element. It is easily shown that the size of the figure is porportional to $T_1 + T_2 + T_3 = Q = M - (2M_{\pi^\pm} + M_{\pi^0})$ Because of the finite width of the peak and the control region, Q varies from event to event, so we use normalized variables, Ti/Q.

a. At first we will take the hypothesis of G-parity conservation in the decay of the ω meson (strong interaction). In this hypothesis, the G parity of the resonance must be the same as that of three pions, i.e., negative. Then there are three possible three-pion resonances with T = 0, J ≤ 1: the vector meson ($1^{--}$), the pseudoscalar meson ($0^{--}$), and the axial meson ($1^{+-}$) (the first super script indicates the parity, the second, G parity). Table VI shows the three possible hypothesis, with their characteristics. The meaning of the angular momenta $\ell$ and L is as follows: the matrix element is analyzed in terms of a single pion plus a dipion, the pions of the dipion are assigned a momentum q and an angular momentum L (in the dipion rest frame), then another pair of variables, p and $\ell$, describes the remaining pion in the rest frame.[25]

Table VI. Possible three-pion resonances with T=0, J≤1, G parity

| Meson | | Matrix element | | | Vanishes at (see Fig. 19) |
|---|---|---|---|---|---|
| Type | J | $\ell$ | L | Simple example | |
| V | $1^{--}$ | 1 | 1 | $(\vec{p}_0 \times \vec{p}_+) + (\vec{p}_+ \times \vec{p}_-) + (\vec{p}_- \times \vec{p}_0)$ | whole boundary |
| PS | $0^{--}$ | 1 and 3 | 1 and 3 | $(E_- - E_0)(E_0 - E_+)(E_+ - E_0)$ | straight lines |
| A | $1^{+-}$ | 0 and 2 | 1 | $E_-(\vec{p}_0 - \vec{P}_+) + E_0(\vec{P}_+ - \vec{P}_-) + E_+(\vec{P}_- - \vec{P}_0)$ | center, b, d, f |

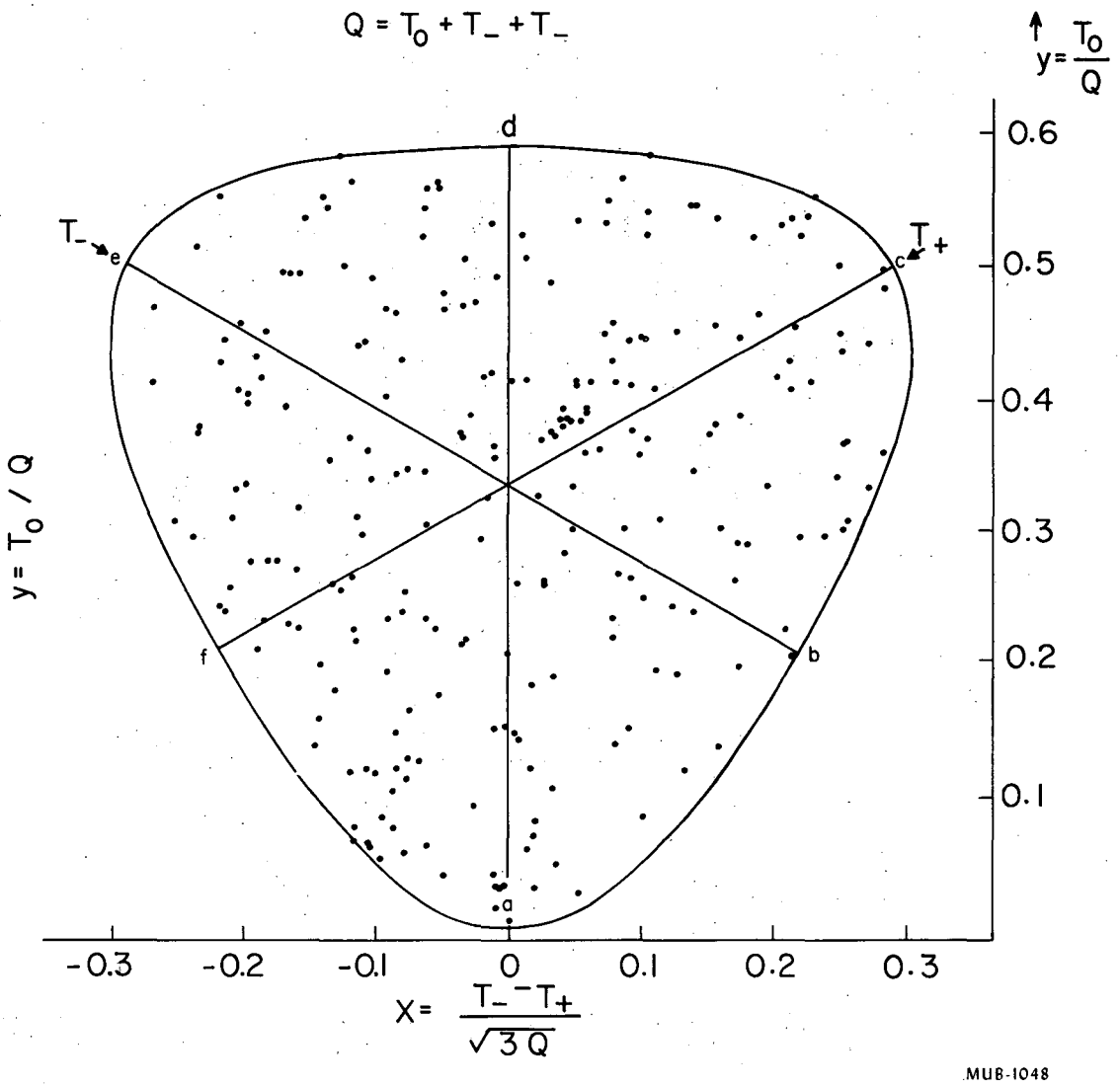


Fig. 20. Dalitz plot for 238 events from the center of the peak region (760 to 800 Mev), 27±8% of which are due to ω mesons. $Q = M_3 - (2M_{\pi^\pm} + M_{\pi^0}) \approx 365$ Mev.

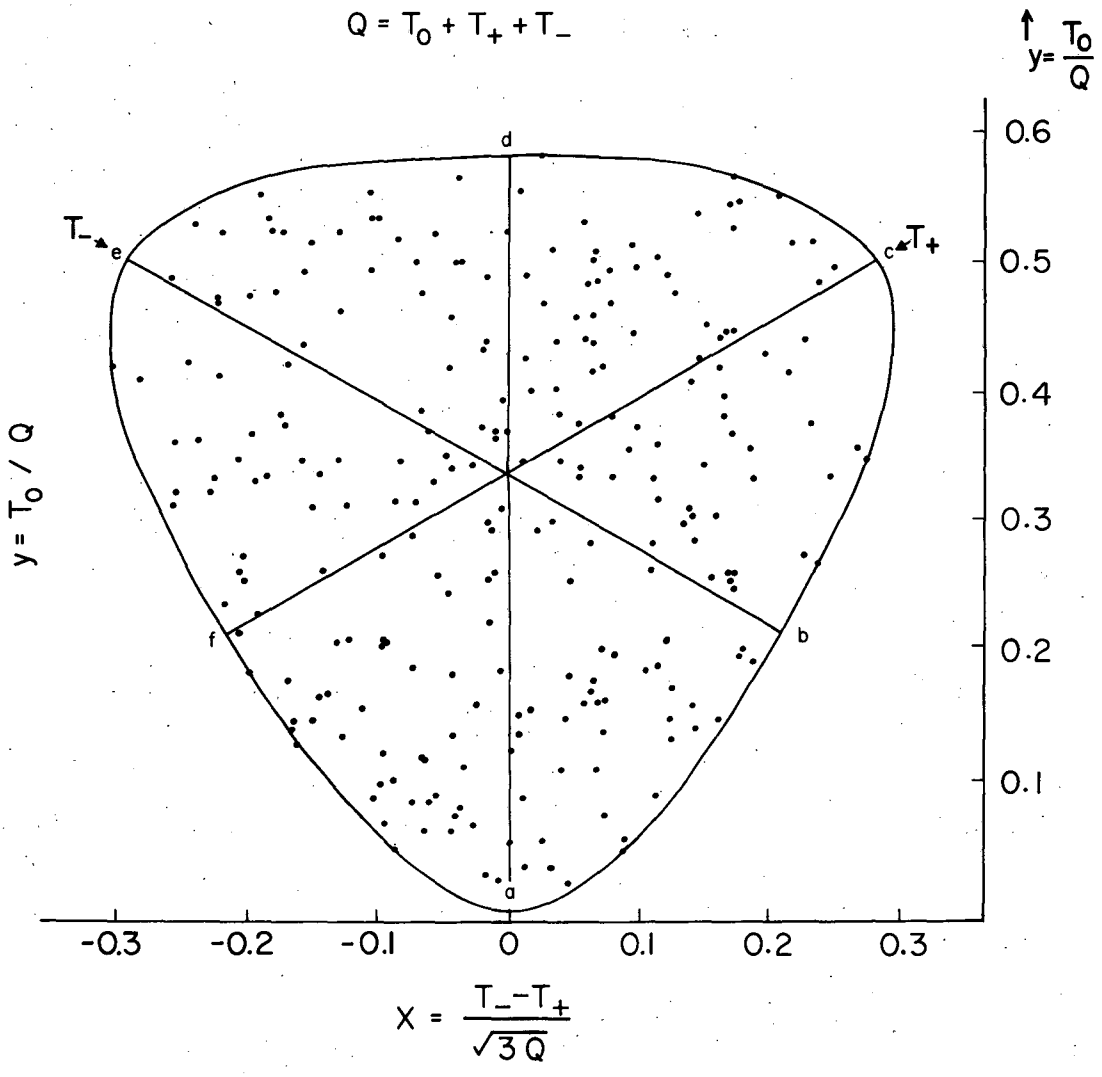


Fig. 21. Dalitz plot for 238 events from the control region (822 to 878 Mev). $Q = M_3 - (2M_{\pi^\pm} + M_{\pi^0}) \approx 435$ Mev.

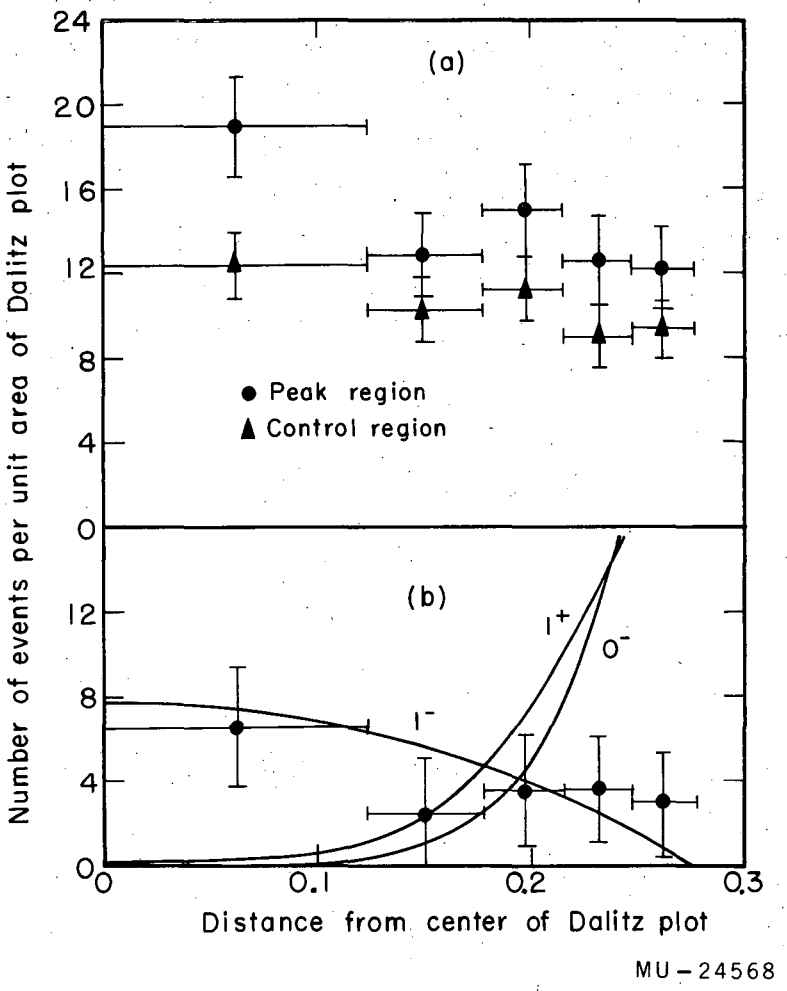


Fig. 22. The density of the population of events on the Dalitz plot for five regions of approximately equal area as a function of the average distance of this region from the center of the Dalitz plot. Both scales are in arbitrary units.
(a) Events in the energy region of the ω meson and in a control region. In the ω peak region there are 238 triplets: 79 omega and 159 background triplets. The number of events per unit area of the control region is normalized to be equal to the estimated background in the peak region.
(b) Difference between the two sets of points in (a) (79 triplets).
The three curves correspond to the predictions for this distribution on the assumptions that the particle has spin and parity $1^{--}$, $1^{+-}$, or $0^{--}$.

In Fig. 22 b are plotted the curves of density of the population of events on the Dalitz plot corresponding to the three possible types of mesons. These curves have been calculated by Stevenson et al.[25] In Fig. 22 a we plot the numbers of events per unit area of the Dalitz plot for the peak region and for the control region versus the distance from the center of the plot. The number of events per unit area of the control region is normalized to be equal to the esimated background in the peak region. Fig. 22 b shows the difference of the two sets of points in Fig. 22 a. We assume that this difference represents the number of events per unit area of the resonance.[26] These data agree very well with the curve predicted by a matrix element of a vector meson($1^{--}$), and not at all with the prediction of a pseudoscalar ($0^{--}$) or axial vector meson ($1^{+-}$).

b. Because the width of the resonance is very small, Duerr and Heisenberg suggest the possibility of electromagnetic decay with non-conservation of G parity.[27] With the present data,[23,25] they can already eliminate many types of mesons except the $1^{++}$, $0^{-+}$, and $1^{--}$ mesons. But as we will see in the next section, the small value of the ratio $R(\omega \to 4\pi/\omega \to \pi^+\pi^-\pi^0)$ and $R(\omega \to /\text{neutral } \pi^+\pi^-\pi^0)$ will eliminate $1^{++}$ and favor strongly the $1^{--}$ spin-parity and G-parity interpretation for the $\omega$ meson.

With the spin and parity ($1^-$) we conclude that the $\omega$ meson can be the particle predicted by Nambu to explain the electromagnetic form factors of the proton and neutron,[6] and also expected in the vector-meson theory of Sakurai,[3] or as a member of an octet of vector mesons, according to the unitary summetry theory.[1] Chew has pointed out that on dynamical grounds such a vector meson can exist as a bound state.[28]

Difference in Mass of the $\omega$ Meson

The value 780 Mev for the mass of the $\omega$ meson (i.e., the center of the resonance) has been determined by the ideogram distribution of the effective mass of the neutral triplets. We estimate an uncertainty of about 5 Mev. This value agrees very well with the one

of Maglić et al. (787 Mev). These two experiments do not involve nucleons in the final state. But Pevsner et al.[23, 29] give the mass of 764 Mev for the meson from the analysis of $\pi^+ + d \rightarrow p + p + \pi^+ + \pi^- + \pi^0$, and Hart et al.[23] get the same mass from the reaction $p + p \rightarrow p + p + \pi^+ + \pi^- + \pi^0$. Their uncertainty must not be more than 5 Mev. This difference of mass can be due to a systematic error in the analysis, or an influence of the presence of nucleon in the final state.

To improve our track reconstruction program, PANG, we have made some slight changes in some parameters (optical constant, magnetic field). This does not affect the value of the mass of the $\omega$ meson. Also, Pevsner et al. use pictures taken from the 72-inch chamber), use the same program (PANG and KICK) for their analysis, and yet find a different $\omega$ mass. It is true that the energy available in the c.m. system is much less in their case than in ours, so that a systematic error can act in different ways.

## C. Effective Mass Distribution of Four Pions

### Motivation for a Search for a Four-Pion Resonance

Since the discovery of the two-pion and three-pion resonances[23, 29, 30] the search for a four-pion resonance has acquired much interest. The interest is threefold:

(a) Chew and Frautschi,[31] using the "Regge poles" theory, predict a possible resonance (or unstable particle) with spin 2 and other quantum numbers those of the "vacuum" (T = 0, parity even) at the region of 1 Bev. This particle could decay into two, four, or six pions. But the four-pion decay could possibly be favored because a two-pion decay would require a d wave, whereas a four-pion decay would need only two pion sets in p wave.

The four-pion resonance could also come from a decay of $\chi^0$, the pseudoscalar meson with I = 0, formulated by many theoreticians.[1, 4]

(b) To the $\omega$ meson has been attributed a spin and parity $1^{--}$ (the first superscript refers to the parity and the second to G parity) if the

decay is through strong interactions. But because of the small width of this meson ($\Gamma/\pi \leq 12$ Mev, and could be zero[23]), Duerr and Heisenberg suggest the possibility of electromagnetic decay with violation of G parity.[27] Four more states will then have to be considered: $0^{++}$, $1^{-+}$, $1^{++}$, and $0^{-+}$ (we consider only states with spin $\leq 1$). Duerr and Heisenberg eliminate the states $0^{++}$ and $1^{-+}$ because their three-pion decay would either not occur or be extremely weak.[27] The three-pion decay of $1^{++}$ or $0^{-+}$ have an uniform density of Dalitz plot, and these assignments cannot be eliminated with the present statistics on Dalitz plots. Therefore, the $\omega$ meson can still have one of the three following spin and parity combinations: $1^{--}$, $0^{-+}$, or $1^{++}$. But Duerr and Heisenberg point out that these three states behave differently with respect to the four-pion decay.[27] For $1^{--}$ the four-pion decay is strongly forbidden, and therefore is completely negligible compared with the three-pion decay. For $0^{-+}$ the four-pion decay is an allowed transition, but reduced to small value by the fact that two D states and one P state are required for the outgoing waves.[27] For $1^{++}$ the four-pion decay is allowed and can be large.[27] Therefore, the very existence of a neutral four-pion resonance at 780 Mev would rule out the $1^{--}$ spin parity; its nonexistence would probably rule out the possibility of the $1^{++}$ spin parity, but not the possibility of the $0^{-+}$ spin parity.

(c) It would also be interesting to see the decay of the $\rho$ meson into four pions. This decay is allowed by strong interaction, but is not as favorable as the two-pion decay. Of special interest is the decay mode $\rho \rightarrow \pi + \eta$, with $\eta \rightarrow \pi^+\pi^-\pi^0$ ($\eta$ being the $I = 0$ 550-Mev, three-pion resonance discovered by Pevsner et al.[30]) Because the G parity of $\rho$ is $+1$ and that of $\pi$ is $-1$, this decay mode of $\rho$ is allowed if the G parity of $\eta$ is $-1$ and forbidden if it is $+1$.

Search for Four-Pion Resonances

For all categories of events we have evaluated the four-body effective mass

$$M_4 = [(E_1 + E_2 + E_3 + E_4)^2 - (\vec{p}_1 + \vec{p}_2 + \vec{p}_3 + \vec{p}_4)^2]^{1/2}$$

for each pion quadruplet.

For the $6\pi$ and $8\pi$ events we can get only the combinations $Q = 0$ (nine quadruplets for each event) and $|Q| = 2$ (six quadruplets for each event). For the $7\pi$ events we can also get the $|Q| = 1$ combination (18 quadruplets for each event).

For the $8\pi$ events we can also calculate the effective mass of two charged pions and two neutral pions by calculating the missing mass of the system consisting of the incoming antiproton, the proton target, and the four remaining visible charged pions:

$$M'_4 = [(E_{\bar{p}} + M_p - E_1 - E_2 - E_3 - E_4)^2 - (\vec{p} - \vec{p}_1 - \vec{p}_2 - \vec{p}_3 - \vec{p}_4)^2]^{1/2}.$$

For $M'_4$, we can form only the $Q = 0$ and $|Q| = 2$ combinations. We calculated for each value of $M_4$ or $M'_4$ an uncertainty $\delta M_4$ or $\delta M'_4$ by using the error matrix calculated by KICK. For the $8\pi$ events the half-width $\Gamma_{res}/2$ of the resolution function of $M_4$ is 13.5 Mev, and for $M'_4$ is 14 Mev. However, because of systematic errors known to exist in our track reconstruction, our estimate of $\Gamma_{res}/2$ probably should be increased by $\sqrt{3}$ to $\Gamma_{res}/2 = 23$ Mev for $M_4$ and $\Gamma_{res}/2 = 24$ Mev for $M'_4$.

For the $6\pi$ and the $7\pi$ events $\Gamma_{res}/2$ is a little smaller.

Figure 23 a is the histogram of the $M_4$ distribution of the $Q = 0$ combination of the $6\pi$ events. The solid-line curve represents the background distribution estimated from the $|Q| = 2$ distribution of the same events (smooth curve drawn through $|Q| = 2$ distribution).

Figure 23 (b) and (c) are the histograms of the $M_4$ distribution of the $7\pi$ events, respectively with $Q = 0$ and $|Q| = 1$. We use the $|Q| = 1$ and $|Q| = 2$ distributions to estimate the background distribution (solid-line curves). In Fig. 23 (d) we renormalize the $|Q| = 1$ distribution of the $7\pi$ events and plot it against the neutral distribution of the same events.

None of these histograms shows any strong disaccord with the background distribution.

In Fig. 24 we plot separately (a) the histogram of the neutral distribution of $M_4(\pi^+\pi^-\pi^+\pi^-)$ and (b) the histogram of the neutral

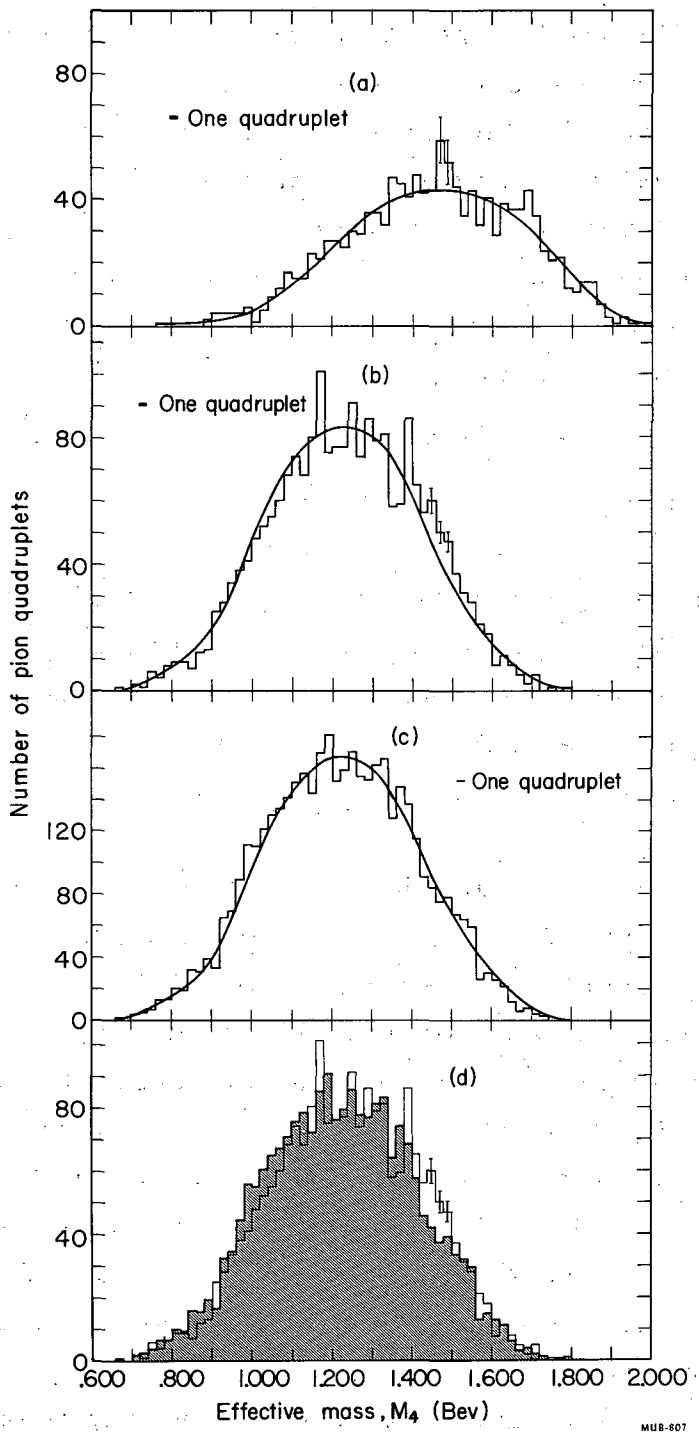


Fig. 23. Histograms of the distributions of the effective masses $M_4$ of pion quadruplets; (a) is for distribution for quadruplets of $6\pi$ events with $Q = 0$ ($153 \times 9$ quadruplets), (b) and (c) for distribution for quadruplets of $7\pi$ events with $Q = 0$ and $|Q| = 1$ respectively ($239 \times 9$ and $239 \times 18$ quadruplets). In (d) the (c) distribution (shaded area) is compared with the (b) distribution.

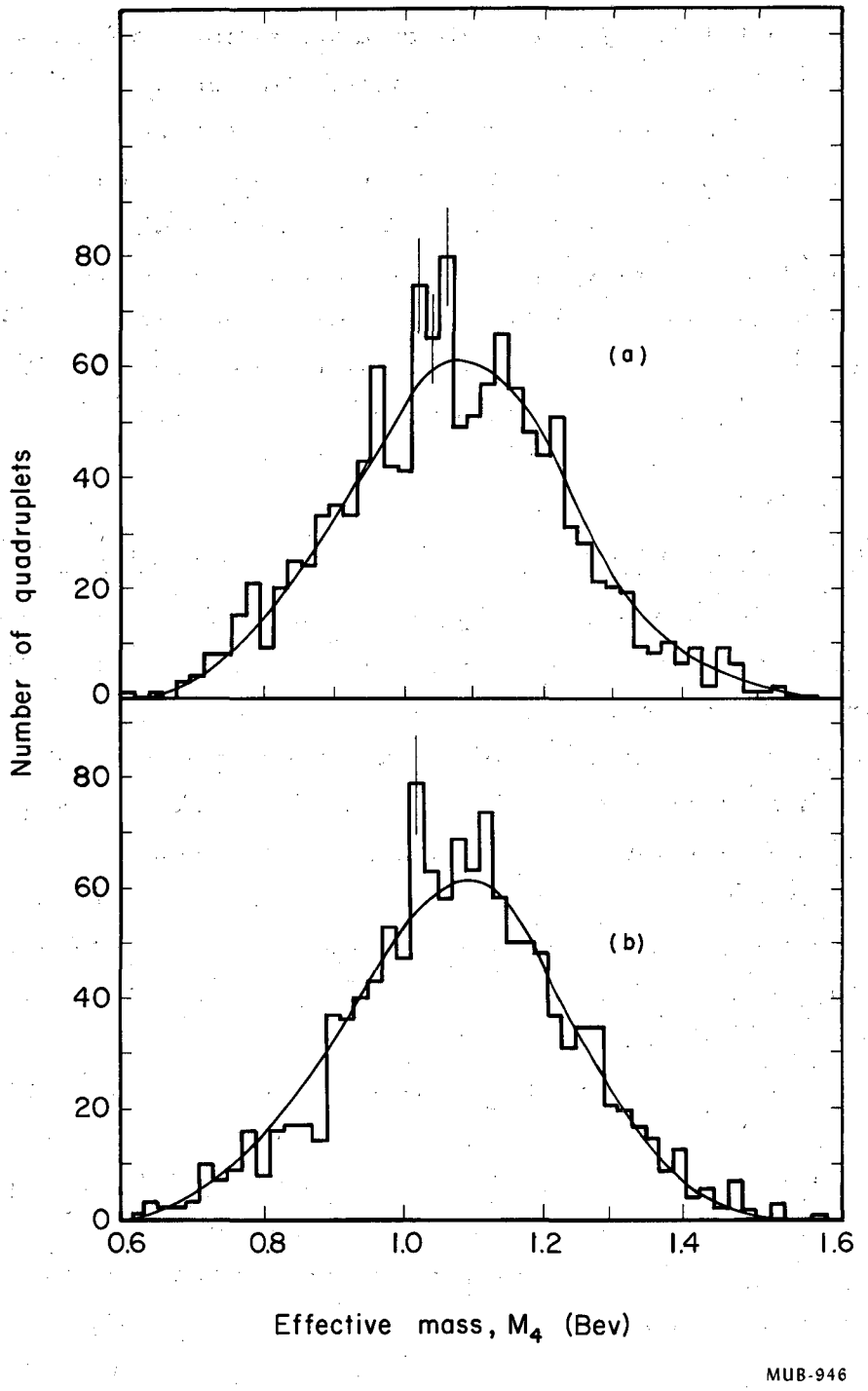


Fig. 24. Histograms of the distributions of the effective masses of neutral pion quadruplets of 8π events; (a) is for distribution of $M_4(\pi^+\pi^+\pi^-\pi^-)$, (139×9 quadruplets), (b) is for distribution of $M_4(\pi^+\pi^-\pi^0\pi^0)$ (139×9 quadruplets). The same smooth curve has been drawn on (a) and (b).

distribution of $M_4^{\prime}$ ($\pi^+\pi^-\pi^0\pi^0$) of the 8 $\pi$ events. The solid-line curves represent the background distribution estimated from a smooth curve drawn through the sum of the distribution of $M_4$ ($\pi^{\pm}\pi^{\pm}\pi^{\pm}\pi^{\mp}$) and of $M'_4$ ($\pi^{\pm}\pi^{\pm}\pi^0\pi^0$) with $|Q| = 2$ of the same events (Fig. 25 a). Figure 25 (b) is the histogram of the sum of the neutral distributions of $M_4$ and $M'_4$.

The neutral $M_4$ distribution shows a suggestive but inconclusive peak at the region of 1.040 Bev. If this peak really exists, it may be a resonance with I = 0 or I = 1. It could come from a possible decay of the $\chi^0$ meson ($I = 0,\ 0^{-+}$) or the particle predicted by Chew and Frautschi ($I = 0,\ 2^{++}$). In the latter meson could also decay into two pions or two kaons. (This particle has been theoretically predicted first by Lovelace but at 400 Mev[31]).

Ratio ($\omega \to 4\pi/\omega \to \pi^+\pi^-\pi^0$) and Spin and Parity of the $\omega$ Meson

To estimate the ratio $R(\omega \to 4\pi/\omega \to \pi^+\pi^-\pi^0)$ we note that we have seen in the same sample of $\bar{p}$-p interactions 79± 18 interactions of the form $\bar{p} + p \to 2\pi^+ + 2\pi^- + \omega$, with $\omega \to \pi^+ + \pi^- + \pi^0$. If the $\omega$ produced by the preceding reaction were to decay by $\omega \to \pi^+ + \pi^- + \pi^0 + \pi^0$ we would see them in our 8 $\pi$ events. But the distribution of $M'_4$ ($\pi^+\pi^-\pi^0\pi^0$) (Fig. 24b) does not show anything over the phase space at the region 780± 20 Mev. At this energy the background is about 26 pion quadruplets; therefore we can estimate a maximum of 10 pion quadruplets that could come from the decay of the $\omega$, and the upper limit of the ratio of $R(\omega \to \pi^+\pi^-\pi^0\pi^0/\omega \to \pi^+\pi^-\pi^0)$ is about 12%.

If the $\omega$ mesons produced by the preceding reaction ($\bar{p} + p \to 2\pi^+ + 2\pi^- + \omega$) were to decay into $2\pi^+ + 2\pi^-$ we would see them in the reaction $\bar{p} + p \to 4\pi^+ + 4\pi^-$. We have only 4± 2 of the latter reactions.[9] This gives a maximum of 5% for $R(\omega \to \pi^+ + \pi^- \pi^+\pi^-/\omega \to \pi^+\pi^-\pi^0)$. We can then conclude that the ratio $R(\omega \to 4\pi/\omega \to \pi^+\pi^-\pi^0)$ is less than 17%, and can very possibly be zero.

If the $\omega$ produced by $\bar{p} + p \to 2\pi^+ + 2\pi^- + \omega$ were to decay in the neutral mode, it would show in the distribution of the missing mass of the reaction $\bar{p} + p \to 2\pi^+ + 2\pi^- + n\pi^0$. By $\omega \to$ neutral, we mean the

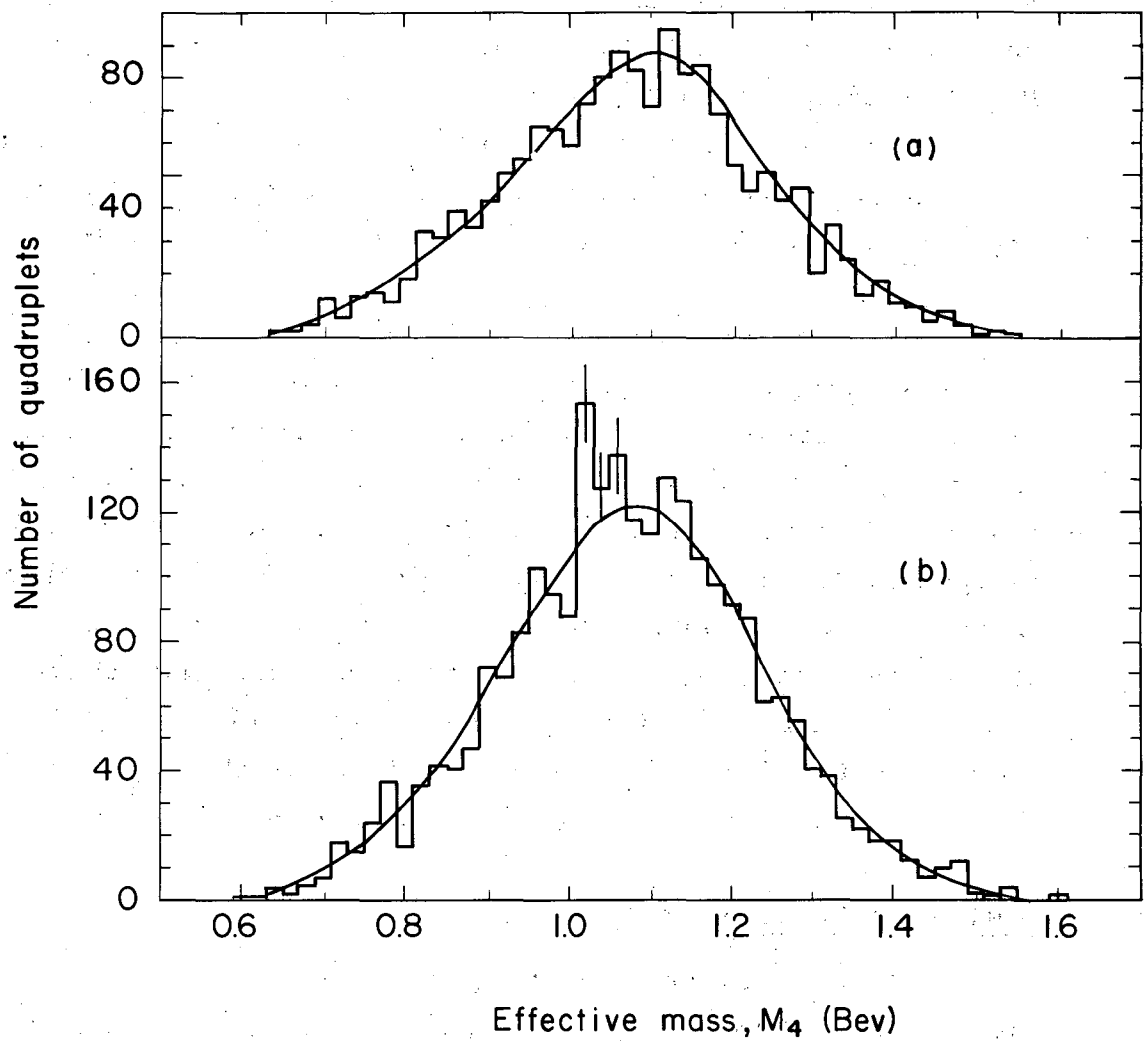


Fig. 25. Histograms of the distributions of the effective masses of pion quadruplets of 8π events; (a) is for distribution of quadruplets with $|Q| = 2$ (139×6 quadruplets), (b) is for quadruplets with $Q = 0$ (139×18 quadruplets). The same smooth curve has been drawn on (a) and (b).

decays $\omega \to 3\pi^0$, $\omega \to 2\gamma$, and $\omega \to \pi^0 + \gamma$. Looking at the latter distribution, J. Button et al. reported seeing no "peak" at the region of 780 Mev,[17] and using our value of 0.6± .15 mb for the cross section of the reaction $\bar{p} + p \to 2\pi^+ + 2\pi^- + \omega$ with $\omega \to \pi^+ + \pi^- + \pi^0$, they estimate $R(\omega \to \text{neutral}/\omega \to \pi^+\pi^-\pi^0) < 0.5$.

The small value of $R(\omega \to 4\pi/\omega \to \pi^+\pi^-\pi^0)$ agrees with a spin and parity assignment of $1^{--}$ and probably rules out the $1^{++}$ assignment, but does not rule out the possibility of $0^-$ for the spin and parity of the $\omega$ meson.[27]

The ratio of $R(\omega \to \text{neutral}/\omega \to \pi^+\pi^-\pi^0)$ is estimated by Duerr and Heisenberg to be larger than 3/2 for the $0^{-+}$ assignment and very small ($10^{-4}$) for the $1^{--}$ assignment.[27] Our values for the two ratios $R(\omega \to 4\pi/\omega \to \pi^+\pi^-\pi^0)$ and $R(\omega \to \text{neutral}/\omega \to \pi^+\pi^-\pi^0)$, which can be very small, agree with the $1^{--}$ assignment and disagree with the $0^{-+}$ assignment for the spin and parity of the $\omega$ meson. Since all other interpretations of spin and parity (with spin $\leq 1$) can be ruled out by the present data,[25] we conclude that the spin and parity of the $\omega$ meson is most probably $1^{--}$. This agrees with the conclusion reached by Stevenson et al.[25] Table VII shows a summary of the experimental determination of spin, parity, and G parity of the $\omega$ meson.

Ratio $(\rho \to 4\pi)/(\rho \to 2\pi)$

To estimate the ratio of $R(\rho \to 4\pi)/(\rho \to 2\pi)$ we use some results from J. Button et al.[17] They find about 386 $\rho^0$ with $\rho^0 \to \pi^+\pi^-$ and about 274 $\rho^\pm$ with $\rho^\pm \to \pi^\pm\pi^0$ by analyzing the reaction $\bar{p} + p \to 2\pi^+ + 2\pi^- + \pi^0$, from a smaller sample of the same $\bar{p}$ picture of our experiment. In our larger sample this would correspond to 482 $\rho^0$ with $\rho^0 \to \pi^+\pi^-$ and 329 $\rho^\pm$ with $\rho^\pm \to \pi^\pm\pi^0$. If the $\rho$ mesons produced by the same mechanism decayed into $\rho^0 \to 2\pi^+ + 2\pi^-$ and $\rho^\pm \to \pi^0 + \pi^+ + \pi^- + \pi^\pm$ we would see them in the $M_4$ distributions of the $7\pi$ events (Fig. 23b; c). In the region around 750 Mev in these distributions we see nothing exceeding phase space and we estimate a maximum of 2% for $R(\rho^0 \to \pi^+\pi^-\pi^+\pi^-/\rho^0 \to \pi^+\pi^-)$ and a maximum of 5% for $R(\rho^\pm \to \pi^\pm\pi^0\pi^+\pi^-/\rho^\pm \to \pi^\pm\pi^0)$. A crude phase-space

Table VII. Summary of experimental determination of spin parity and G parity of $\omega$ meson (I=0, $M_{\pi^+\pi^-\pi^0} = 780$ Mev).

| Possible assignment (Spin $\leq 1$, parity, G parity) | Eliminated by |
|---|---|
| $0^{--}$ | Dalitz plot |
| $0^{+-}$ | Parity conservation |
| $\boxed{1^{--}}$ | |
| $1^{+-}$ | Dalitz plot |
| $0^{-+}$ | Dalitz plot and small ratio $R(\omega \to \text{neutral}/\omega \to \pi^+\pi^-\pi^0)$ |
| $0^{++}$ | Parity conservation |
| $1^{-+}$ | Small ratio $R(\omega \to 4\pi/\omega \to \pi^+\pi^-\pi^0)$ |
| $1^{++}$ | Dalitz plot, small ratio $R(\omega \to 4\pi/\omega \to \pi^+\pi^-\pi^0)$ and small ratio $R(\omega \to \text{neutral}/\omega \to \pi^+\pi^-\pi^0)$ |

calculation predicts for $R(\rho \to 4\pi/\rho \to 2\pi)$ a value of $\lambda^2/4$, where $\lambda = \Omega/\Omega_0$, $\Omega$ being the interaction volume of the $\rho$ meson and $\Omega_0 = (4\pi/3)(\hbar/m_\pi c)^3$. Thus an experimental ratio $R \leq 5\%$ would give $\lambda \leq 0.5$ for the $\rho$ meson.

To estimate the ratio $R(\rho^\pm \to \pi^\pm + \eta, \eta \to \pi^+\pi^-\pi^0/\rho^\pm \to \pi^\pm\pi^0)$ we analyze carefully all the $|Q| = 1$ quadruplets with effective mass $M_4$ in the region 750±50 Mev (41 quadruplets). In particular we compare the $Q = 0$ distribution of the effective mass of three pions $M_3(\pi^+\pi^-\pi^0)$ coming from these quadruplets with that for $|Q| \leq 1$, ($\pi^\pm\pi^\pm\pi^\mp$ and $\pi^\pm\pi^\pm\pi^0$) (the latter is used here as an estimated background). In the region 548± 10 Mev we have 19 neutral triplets and 15 charged triplets. This

enables us to estimate the number of $\rho^{\pm} \to \pi^{\pm} + \eta$ with $\eta \to \pi^+\pi^-\pi^0$ to be $4 \pm 6$, and the ratio $R(\rho^{\pm} \to \pi^{\pm} + \eta,\ \eta \to \pi^+\pi^-\pi^0 / \rho^{\pm} \to \pi^{\pm}\pi^0)$ to be $1.2 \pm 2.0\%$. This result agrees very well with that of Rosenfeld et al., who find $R(\rho^{+} \to \pi^{+} + \eta,\ \eta \to \text{neutral} / \rho^{+} \to \pi^{+}\pi^0) \leq 0.6\%$.[32] The actual data on the $\eta$ meson seem to rule out all spin parity assignments except $1^{--}$ and $0^{-+}$. The theoretical ratio $R(\rho \to \pi + \eta / \rho \to \pi\pi)$ is very small (i.e., proportional to $(e^2/\hbar c)^2$) for $0^{-+}$. For $1^{--}$, this ratio is not yet well determined (25% for a simple phase-space calculation,[31] 1% after Glashow and Sakurai[33]). We conclude that the small value of the ratio $R(\rho \to \pi + \eta / \rho \to \pi + \pi)$ agrees with the $0^{-+}$ assignment for the spin, parity, and G parity of the $\eta$ meson; whether or not this can rule out the $1^{--}$ assignment depends on a more precise calculation.

D. Effective-Mass Distribution of Five Pions

The interest in a five-pion resonance is twofold:

(a) it could come from the decay of $\pi'$ mesons, a scalar meson ($0^{+-}$) with isotopic spin I = 1;

(b) it would be interesting to know the ratio of $(\omega \to 5\pi / \omega \to \pi^+\pi^+\pi^0)$. The decay $(\omega \to 2\pi^+ + 2\pi^- + \pi^0)$ is allowed by strong interaction but is not as favorable as $(\omega \to \pi^+ + \pi^- + \pi^0)$, by phase-space considerations.

We have evaluated the five-pion effective mass for each type of event:

$$M_5 = \left[ (E_1 + E_2 + E_3 + E_4 + E_5)^2 - (\vec{p}_1 + \vec{p}_2 + \vec{p}_3 + \vec{p}_4 + \vec{p}_5)^2 \right]^{1/2}.$$

The $6\pi$ and $8\pi$ events can yield only the combination with total charge $|Q| = 1$. The distributions of these quintuplets are quite smooth. Each $7\pi$ event can yield 21 quintuplets corrsponding to the charge states

| | | |
|---|---|---|
| $Q = 0$, | $\pi^+\pi^+\pi^-\pi^-\pi^0$, | (nine combinations) |
| $\lvert Q \rvert = 1$, | $\pi^{\pm}\pi^{\pm}\pi^{\pm}\pi^{\mp}\pi^{\mp}$, | (six combinations) |
| $\lvert Q \rvert = 2$, | $\pi^{\pm}\pi^{\pm}\pi^{\pm}\pi^{\mp}\pi^0$ | (six combinations) |

Figure 26 (a, b, c) shows the histogram of the distributions of $M_5$ of $7\pi$ events with $Q = 0$, $|Q| = 1$, and $|Q| = 2$, respectively. The

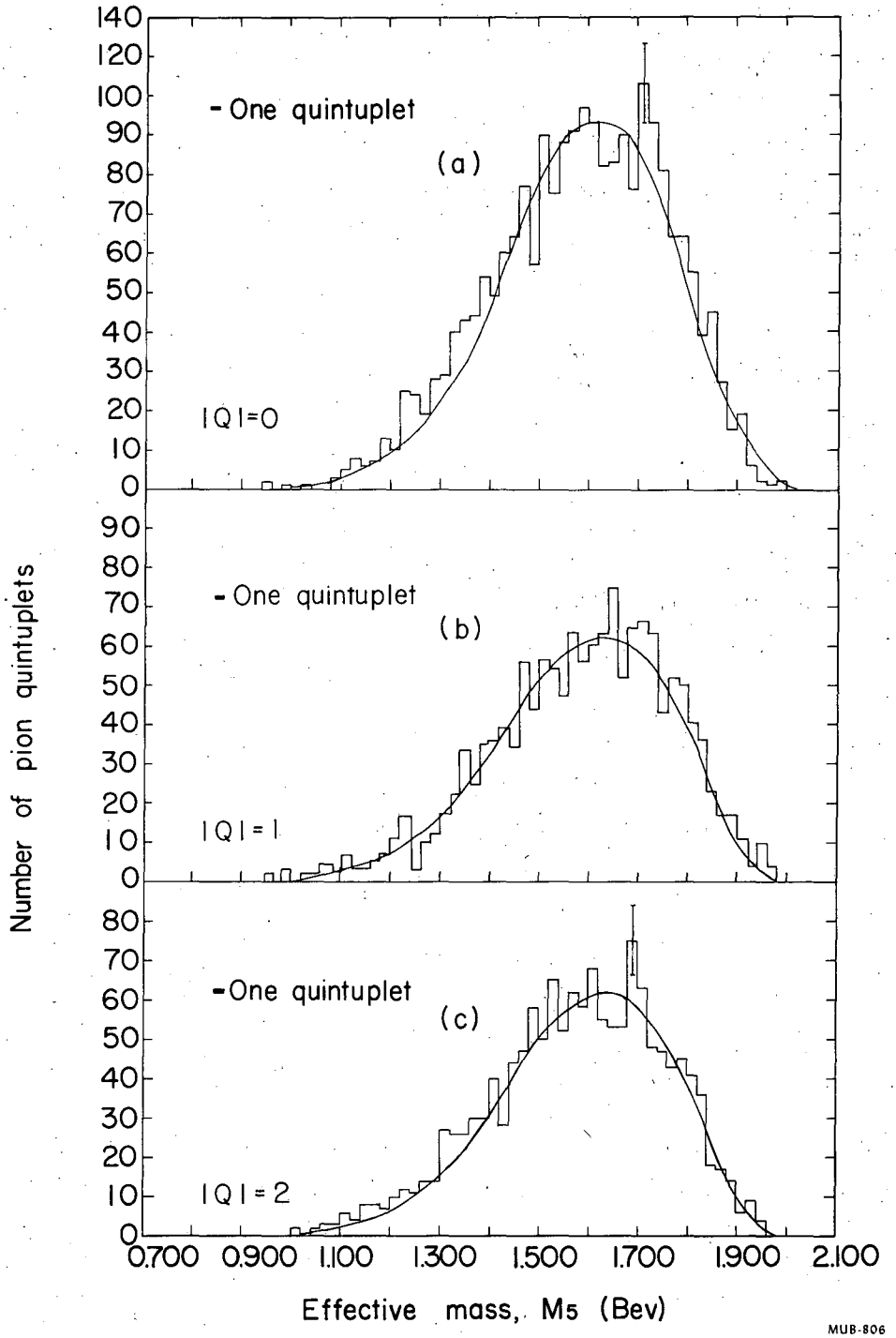


Fig. 26. Histograms of the distributions of the effective masses of pion quintuplets of $7\pi$ events; (a) with $Q = 0$ ($239 \times 9$ quintuplets) (b) with $|Q| = 1$ ($239 \times 6$ quintuplets); (c) with $|Q| = 2$ ($239 \times 6$ quintuplet.) The same smooth curve has been drawn on (a), (b), and (c).

smooth curves represent the background distribution estimated from a smooth curve drawn through the $|Q| = 2$ distribution. These distributions do not show any significant deviation from the estimated background.

This does not mean that the $\pi'$ meson does not exist. Because in one event we can form many pion quintuplets, our efficiency of detecting new resonances is very poor. (For example, we can form 15 quintuplets with $Q = 0$ or $|Q| = 1$, but obviously, only one quintuplet can come from the $\pi'$ meson).

To estimate the ratio $R(\omega \to 2\pi^+ + 2\pi^- + \pi^0 / \omega \to \pi^+ + \pi^- + \pi^0)$ we note that Maglić et al.[22,24] have reported seeing 130±20 interactions of the form $\bar{p} + p \to \omega + \pi^+ + \pi^-$ with $\omega \to \pi^+ + \pi^- + \pi^0$ in the same sample of $\bar{p}$-p interaction. If the mesons produced by the preceding interaction decayed by $\omega \to 2\pi^+ + 2\pi^- + \pi^0$, we would see them in our $7\pi$. But the distribution of $M_5(\pi^+\pi^+\pi^-\pi^-\pi^0)$ of the $7\pi$ events (Fig. 26a) does not show anything at the region 780±20 Mev, and we can estimate a maximum of 1% for the ratio $R(\omega \to 2\pi^+ 2\pi^- 2\pi^0 / \omega \to \pi^+\pi^-\pi^0)$. This result agrees very well with the prediction from a crude Lorentz-invariant phase-space calculation which gives a value of $\lambda^2/3000$ for this ratio, where $\lambda = \Omega/\Omega_0$, $\Omega$ being the interaction volume of the $\omega$ meson and $\Omega_0 = (4\pi/3)(\hbar/m_\pi C)^3$. For $R < \frac{1}{100}$, $\lambda < 5.4$, which is expected.

## E Effective Mass Distribution of Two Pions, and Angular Correlations

For every event we have evaluated the two-pion effective mass,

$$M_2 = [(E_1 + E_2)^2 - |\vec{p}_1 + \vec{p}_2|^2]^{1/2}.$$

The $6\pi$ and $8\pi$ events can yield only pion pairs with charge $Q = 0$ $(\pi^+\pi^-)$ and $|Q| = 2$ $(\pi^\pm\pi^\pm)$ (nine and six combinations respectively, per event). The $7\pi$ events can also yield pairs with charge $|Q| = 1$ $(\pi^\pm\pi^0)$ (six combinations per event). We calculated for each value of $M_2$ an uncertainty $\delta M_2$ by using the error matrix propagated by KICK. After correction for the systematic errors known to exist in our track reconstruction we get, for the half width of the resolution function of $M_2$,

$\Gamma_{res}/2$ = 7 Mev for a pair of two visible pions ($\pi^+\pi^-$ or $\pi^\pm\pi^\pm$), and $\Gamma_{res}/2$ = 14 Mev for a pair of one visible pion and one neutral pion ($\pi^\pm\pi^0$).

The difference in the resolution function of $M_2$ comes from the fact that the momentum and direction of a charged--therefore "visible"--pion can be measured, i.e., be precisely known. The fitting process reduces the uncertainty only slightly. But the momentum and direction of a neutral pion are given only by the conservation of momentum and of energy in the fitting process with much bigger uncertainty (for example, $\Delta p/p \approx 2\%$ for a charged pion; it is 10% for a neutral pion).

As Goldhaber et al.[34] have done, we calculated for each pion pair the angle between the two pions in the center of mass of the anti-proton-proton system:

$$\cos\theta_{12} = \vec{P}_1 \cdot \vec{P}_2 / |P_1| \cdot |P_2| \quad .$$

We also calculated for each pion pair the decay angle of the pion in the rest frame of the dipion.

The 6 $\pi$ events ($\bar{p} + p \rightarrow 3\pi^+ + 3\pi^-$) are the best ones to be investigated for a possible two-pion resonance. They cannot have the T = 0 three-pion resonance, and-- as we have seen--they do not show any significant peak in their three-and four-pion effective-mass distributions. About one-third of the 7 $\pi$ events ($\bar{p} + p \rightarrow 3\pi^+ + 3\pi^- + \pi^0$) would go by the reaction ($\bar{p} + p \rightarrow 2\pi^+ + 2\pi^- + \omega$) and can complicate the interpretation of the effective-mass distribution of two pions of these events. Of the 8 $\pi$ events ($\bar{p} + p \rightarrow 3\pi^+ + 3\pi^- + 2\pi^0$), as we discuss below, we expect a large fraction to go by the reaction $\bar{p} + p \rightarrow \pi^+ + \pi^- + 2\omega$.

Therefore in the following paragraphs we examine the 6 $\pi$ events in much greater detail than the 7 $\pi$ and 8 $\pi$ events.

6 $\pi$ Events

Figure 27 is the histogram distribution of the $M_2$ for the effective mass of pion pairs of the 6 $\pi$ events. In Fig. 27 (a) we plot the Q = 0 combination, in Fig. 27 (b), the |Q| = 2 combination. The solid curves

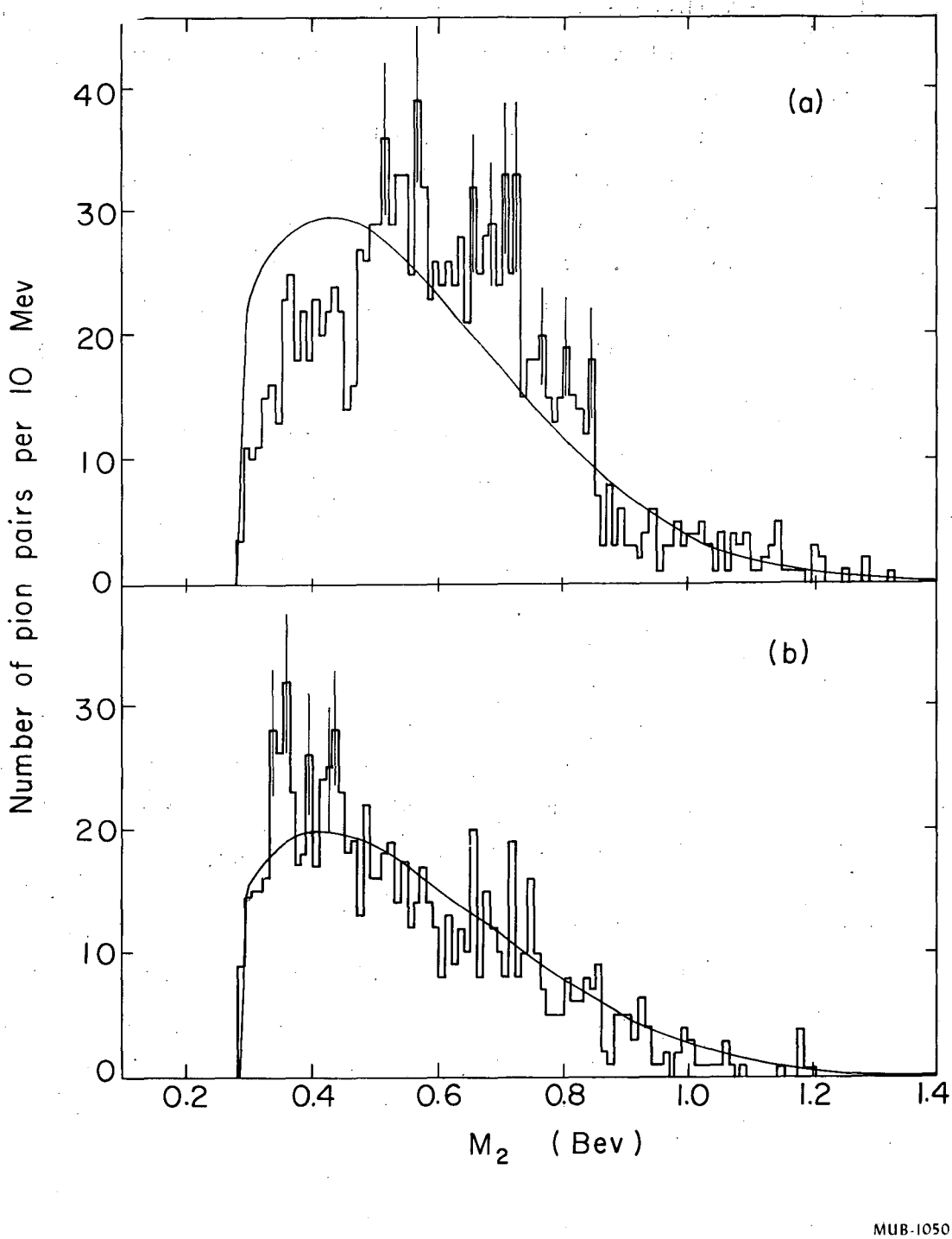


Fig. 27. Histograms of the distributions of the effective masses of pion pairs of 6π events; (a) with $Q = 0$ (153×9 pairs); (b) with $|Q| = 2$ (153×6 pairs). The solid curves are from the Lorentz-invariant phase-space calculation.

represent the Lorentz-invariant phase-space calculation.[35]

In Fig. 28 is an alternative way of displaying effective-mass correlations. It shows the distribution of angles between pion pairs from 6 $\pi$ events as a function of $\cos\theta_{\pi\pi}$ for $Q = 0$ (or unlike pair, $\pi^+\pi^-$) and $|Q| = 2$ (or like pair, $\pi^\pm\pi^\pm$) respectively. The solid curves (identical except for normalization) correspond to calculations on the Lorentz-invariant phase-space model;[34] their slopes simply reflect conservation of momentum.

Figures 29, 30, and 31 are the decay-angle distributions of one pion in the dipion rest frame, (a) for $Q = 0$ and (b) for $|Q| = 2$. The three figures correspond to three regions of $M_2$, Fig. 29 for $M_2$ between 280 and 460 Mev, Fig. 30 for $M_2$ between 500 and 600 Mev, and Fig. 31 for $M_2$ between 600 and 800 Mev.

The most striking result seen in these 6 $\pi$ figures is in Fig. 27, namely, the big difference between the neutral $M_2$ distribution and the $|Q| = 2$ $M_2$ distribution between 280 and 460 Mev. In this effective-mass range the $|Q| = 2$ distribution is above the phase space and the $Q = 0$ distribution is well below. The decay-angle distributions of those dipions (Fig. 29a and b) look the same for $Q = 0$ and $|Q| = 2$ pairs (unlike and like pairs). Both seem to peak at $\cos\phi = 0$ and decrease at $\cos\phi = \pm 1$. The alternative distribution of angles between all the pion pairs (Fig. 28 a and b ) also deviates strongly from the phase-space calculation. The angle between the unlike pions ($Q = 0$) is bigger than the value predicted by phase-space calculation. The phase-space calculation predicts a value of 1.7 for the ratio $\gamma$ = (number of pion pairs with angle $>90°$)/(number of pion pairs with angle $<90°$), whereas we observe $\gamma = 2.45 \pm .1$ for unlike pions. The angle between the like pions ($Q = 2$) is found to be smaller than the value predicted by phase-space calculation, $\gamma = 0.92 \pm .07$. It is interesting to compare our results with the results of the analysis of four-prong events from the same experiment. Button et al. do not seem to observe this striking difference between the $Q = 0$ and $|Q| = 2$ distribution at the region of $M_2$ between 280 and 460 Mev.[17] Looking at the reaction

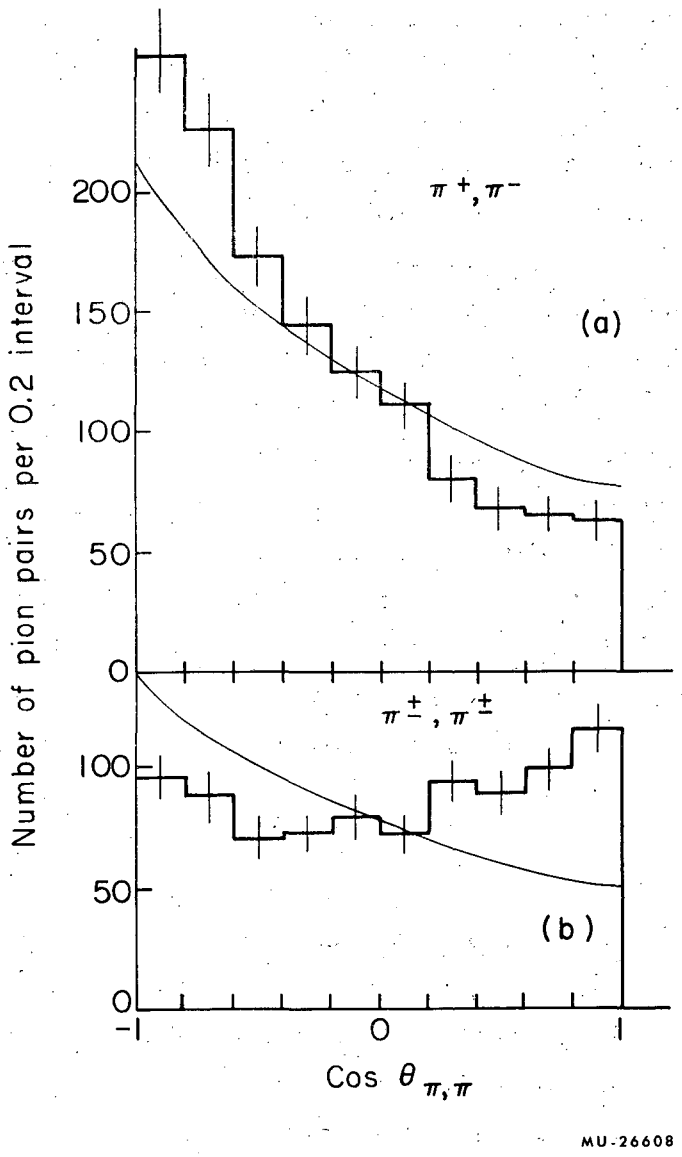


Fig. 28. Distribution of angle between pion pairs from 6π events as a function of cos $\theta_{\pi\pi}$; (a) for pairs ($\pi^+\pi^-$) with $Q = 0$ (153×9 pairs); (b) for pairs ($\pi^\pm\pi^\pm$) with $|Q| = 2$ (153×6 pairs). The solid curves correspond to the Lorentz-invariant phase-space calculation.

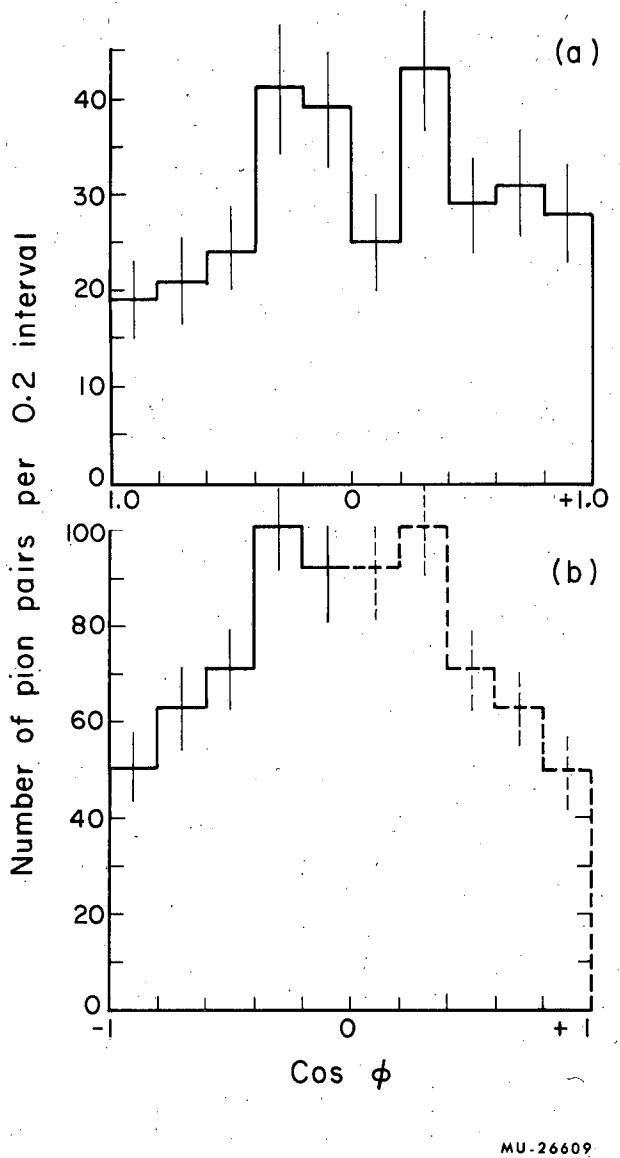


Fig. 29. Distribution of decay angle of one pion in the rest frame of a dipion from "6π" events with effective mass $M_2$ between 280 and 460 Mev (a) for $\pi^+$ from a $\pi^+\pi^-$ dipion (b) for $\pi^\pm$ from a $\pi^\pm\pi^\pm$ dipion (symmetrized).

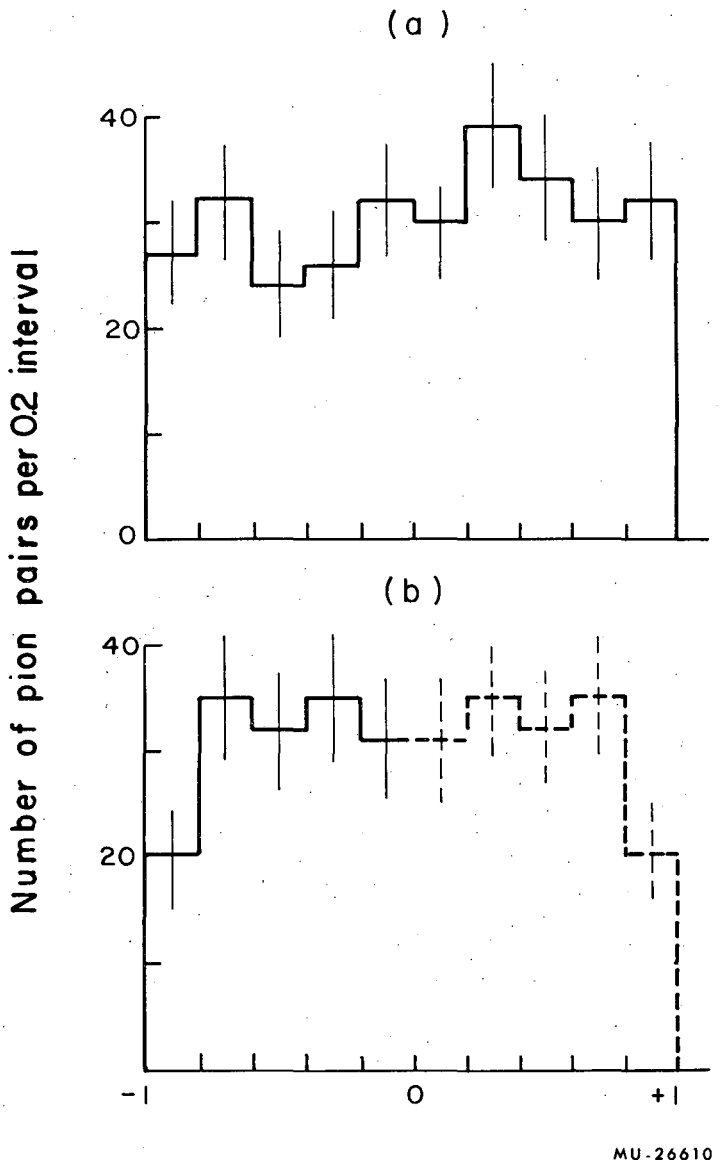


Fig. 30. Distribution of decay angle of one pion in the rest frame of a dipion from 6π events with effective mass $M_2$ between 500 and 600 Mev (a) for $\pi^+$ from a $\pi^+\pi^-$ dipion (b) for $\pi^\pm$ from a $\pi^\pm\pi^\pm$ dipion (symmetrized).

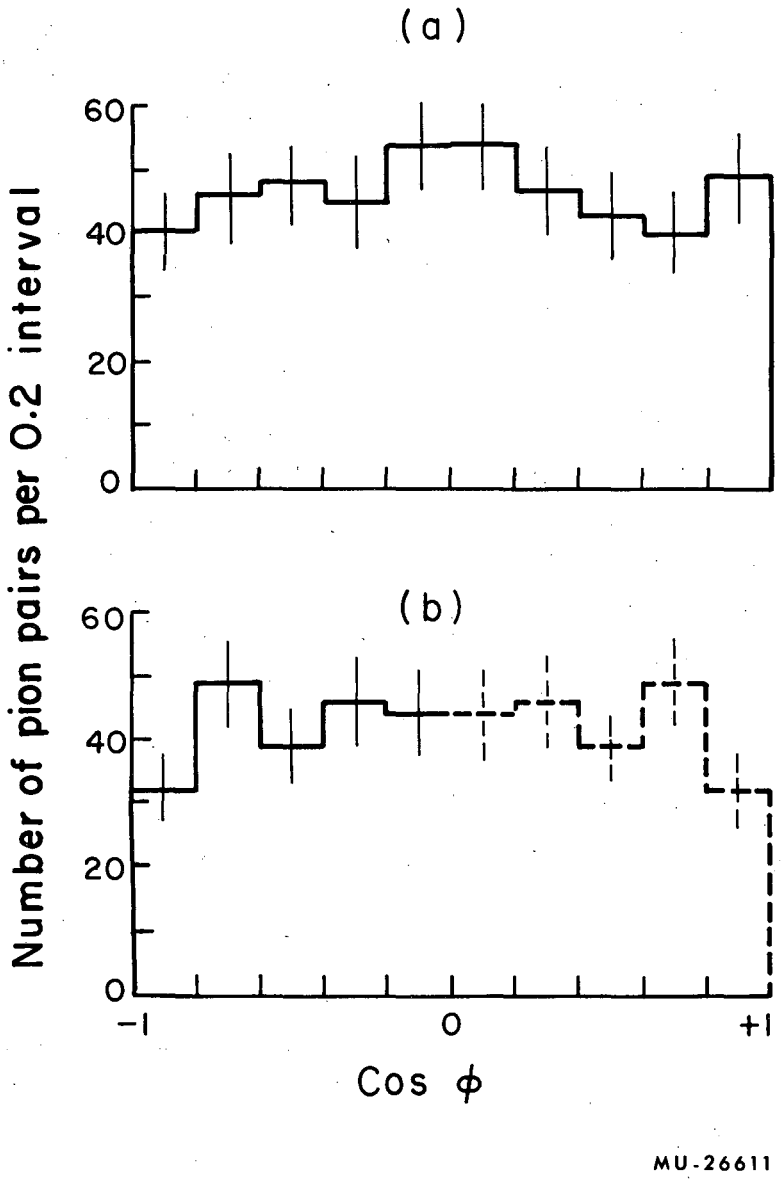


Fig. 31. Distribution of decay angle of one pion in the rest frame of a dipion from 6π events with effective mass $M_2$ between 600 and 800 Mev (a) for $\pi^+$ from a $\pi^+\pi^-$ dipion (b) for $\pi^\pm$ from a $\pi^\pm\pi^\pm$ dipion (symmetrized).

$\bar{p} + p \rightarrow 2\pi^+ + 2\pi^- + \pi^0$ of the same experiment, Maglić et al.[20] report $\gamma = 1.56 \pm .08$ for like pions against $\gamma = 1.79$ predicted by phase space. But they attribute part of this effect to the asymmetry observed in the angular distribution of charged pions in the $\bar{p}$-p center of mass. It is also interesting to compare our results with those of Lee et al.,[36] who analyze the reaction $\bar{p} + p \rightarrow 2\pi^+ + 2\pi^- + \pi^0$ from $\bar{p}$-p annihilation at rest. They find a definite difference in the distribution of $M_2$ of the pion pair for like and unlike: low values of $M_2$ are enhanced for like pion pairs. Also they find a difference between the angular distributions of like-andunlike-pion pairs ($\gamma_{unlike} = 2.26 \pm .15$, $\gamma_{like} = 1.14 \pm .10$), even though they do not have any asymmetry in the angular distribution of pions in the $\bar{p}$-p center-of-mass system. Possibly the difference and similarity of results reflect the fact that the average energy available for each pion for our 6 $\pi$ event ($E_\pi = 2290/6 = 382$ Mev) is less than in the $\bar{p} + p \rightarrow 2\pi^+ + 2\pi^- + \pi^0$ event of Maglić et al. ($E_\pi = 2290/5 = 458$ Mev), but about the same as in the $\bar{p} + p \rightarrow 2\pi^+ + 2\pi^- + \pi^0$ at rest ($E_\pi = 1880/5 = 396$ Mev).

We cannot attribute the differences between the distributions of $M_2$ in the region 280 to 460 Mev and in the angular-correlation distribution between unlike ($Q = 0$) and like ($|Q| = 2$) pion pairs to the asymmetry of angular distribution of pions in the $\bar{p}$-p center of mass, because we do not observe any asymmetry (see Fig. 14) also, the c.m. angular distribution is the same for $\pi^+$ and $\pi^-$.

These differences seem to be best explained by the influence of the Bose-Einstein statistics for pions, as suggested by Goldhaber et al.[37] The Bose-Einstein effect acts like a weak attraction between like pions and a weak repulsion between unlike pions. This would favor small angles for the like-pion pair, and therefore enhance the lower part of their effective-mass distribution (Fig. 27 b). This would also favor large angles for the unlike-pion pair and therefore depopulate the lower part of their effective-mass distribution (Fig. 27 a). Goldhaber et al. have estimated the Bose-Einstein effect on the reaction $\bar{p} + p \rightarrow 2\pi^+ + 2\pi^- + n\pi^0$ with $n = 0$, 1, and 2.[37] The corresponding

calculation for the reaction $\bar{p} + p \rightarrow 3\pi^+ + 3\pi^-$ is more complicated and has not been done. But with a maximum of three like pions instead of two like pions in the $\bar{p} + p \rightarrow 2\pi^+ + 2\pi^- + \pi^0$ reaction, we expect the Bose-Einstein effect to be greater in the reaction $\bar{p} + p \rightarrow 3\pi^+ + 3\pi^-$. And this seems to be verified by our results.

At the higher region of $M_2$ ($M_2 > 500$ Mev) the $|Q| = 2$ distribution follows well the phase-space calculation but the $Q = 0$ ($\pi^+\pi^-$) distribution disagrees completely with the phase space calculation (Fig. 26 (a) and (b)). This effect is probably due to $\rho$ mesons which can decay into $\pi^+\pi^-$ but not $\pi^\pm\pi^\pm$.

7π and 8π Events

Figure 32 shows histograms of distribution of the effective mass $M_2$ of the $Q = 0$, $|Q| = 1$, and $|Q| = 2$ pion pairs from the 7π events. Figure 33 shows distributions of the angle between the $Q = 0$, $|Q| = 1$, and $|Q| = 2$ pion pairs from the same events.

The effective-mass distributions still show a difference at the region of lower value of $M_2$ (280 to 460 Mev) between the like-pion pairs ($|Q| = 2$, $\pi^\pm\pi^\pm$) and the unlike-pion pairs ($Q = 0$, $\pi^+\pi^-$ or $|Q| = 1$, $\pi^\pm\pi^0$). Also at the higher regions of $M_2$ (500 to 800 Mev) the $|Q| = 2$ distribution agrees well with phase space and the neutral distribution seems to show an almost continuous enhancement above phase space.

Figure 34 shows histograms of the distribution of $M_2$ for $Q = 0$ and $|Q| = 2$ pion pairs from the 8π events. The solid curves are the Lorentz-invariant phase-space estimations. Figure 35 shows the distribution of angle between $Q = 0$ and $|Q| = 2$ pion pairs from the same events as a function of $\cos\theta_{\pi\pi}$.

Both the $Q = 0$ and $|Q| = 2$ effective-mass distribution agree with the phase-space estimation. Also the angle correlations are almost the same for unlike ($Q = 0$) and like ($|Q| = 2$) pairs ($\gamma_{\text{unlike}} = 1.55 \pm .07$, $\gamma_{\text{like}} = 1.40 \pm .08$.)

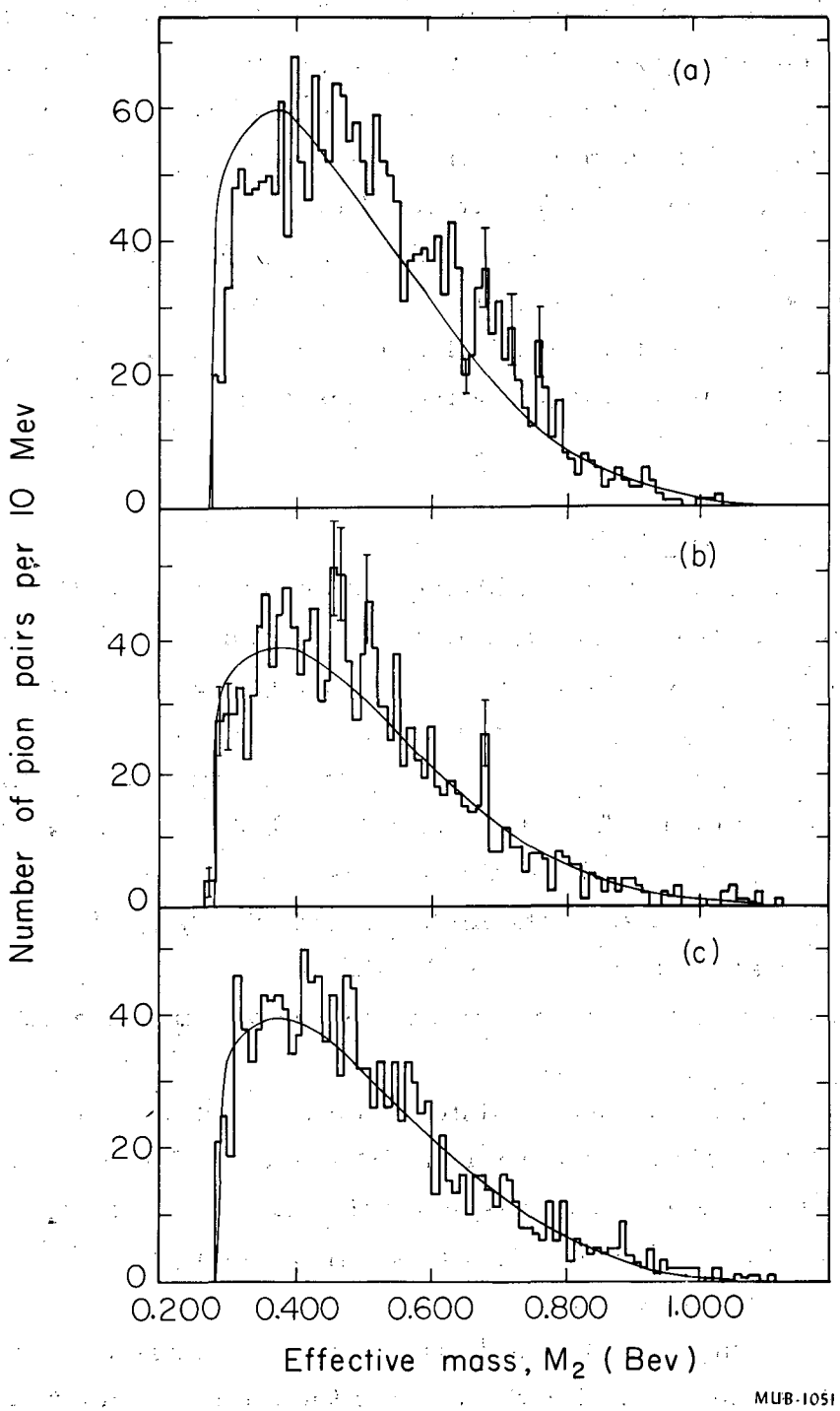


Fig. 32. Histograms of the distribution of the effective mass of pion pairs of "7π" events (a) with Q = 0 (239×9 pairs); (b) with |Q| = 1 (239×6 pairs); (c) with |Q| = 2 (239×6 pairs). The solid curves correspond to a Lorentz invariant phase space calculation.

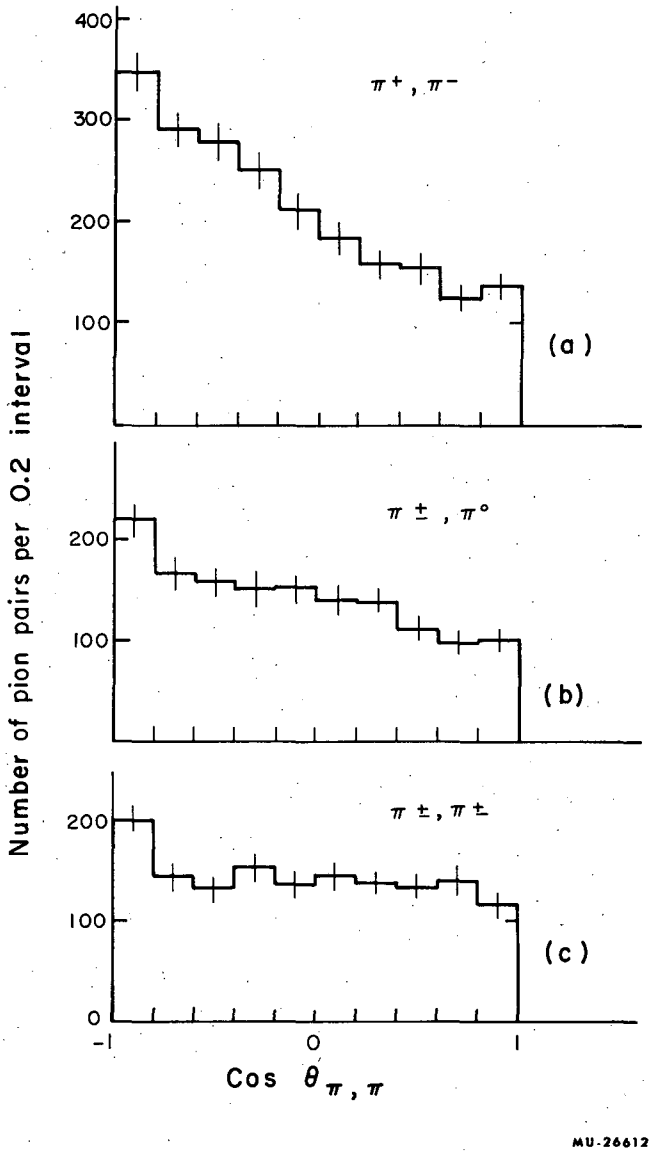


Fig. 33. Distribution of angle between pion pairs from "7π" events as a function of $\cos\theta_{\pi\pi}$ (a) for $Q = 0$ pairs ($\pi^+\pi^-$) (239×9 pairs); (b) for $|Q| = 1$ pair ($\pi^\pm\pi^0$)(239×6 pairs); (c) for $|Q| = 2$ pairs ($\pi^\pm\pi^\pm$) (239×6 pairs).

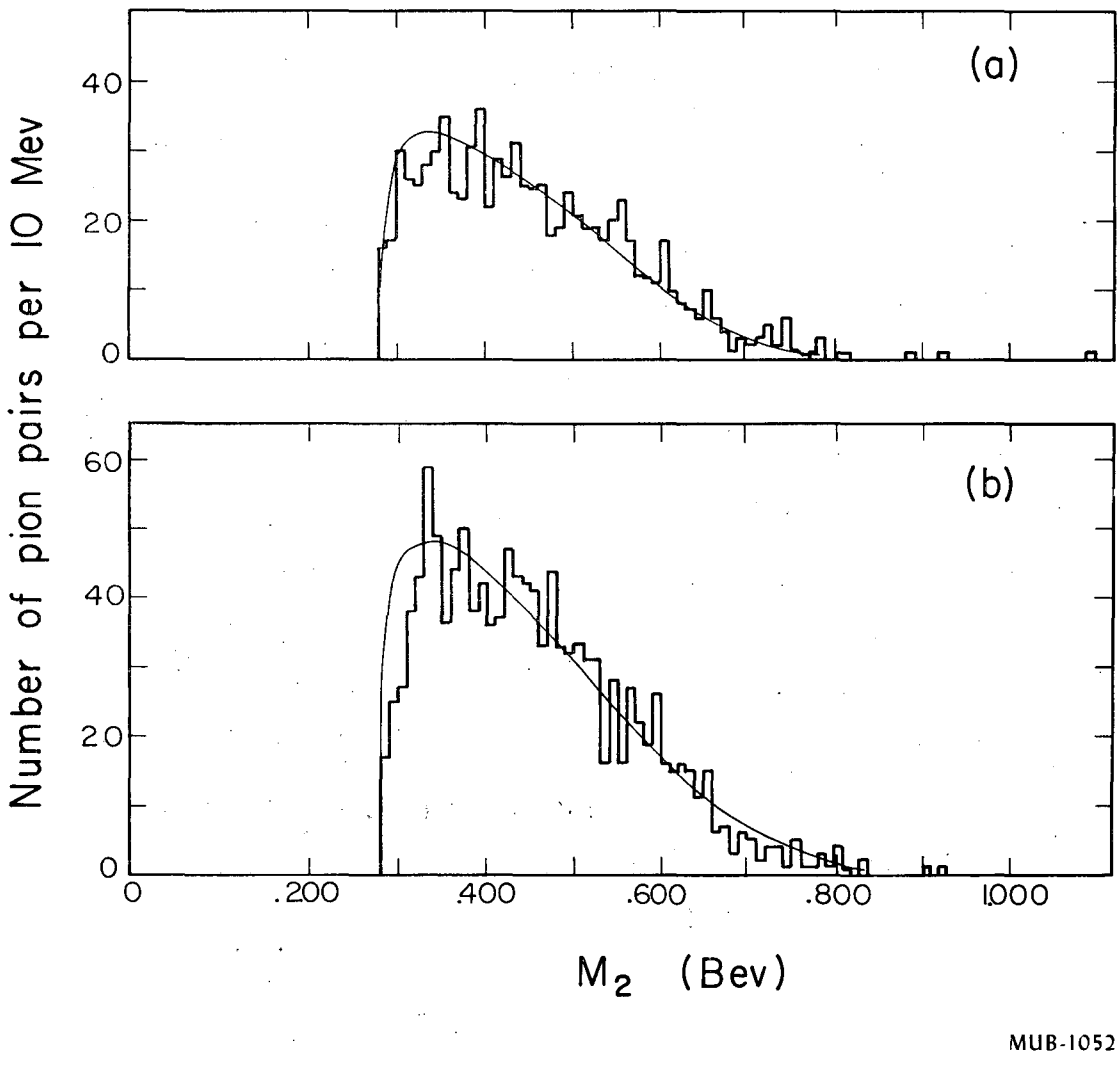


Fig. 34. Histogram of the distribution of the effective mass of pion pairs of "8π" events (a) with Q = 0 (139×9 pairs); (b) with Q = 2 (139×6 pairs). The solid curves is an estimation of Lorentz phase space prediction.

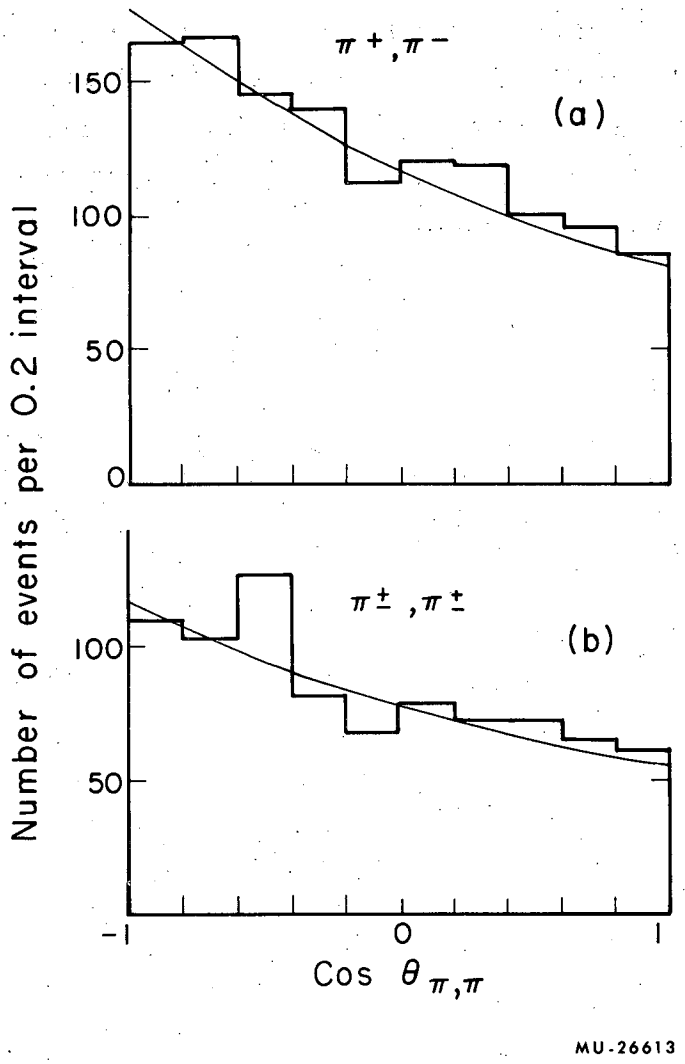


Fig. 35. Distribution of angle between pion pairs from "8π" events as a function of cos $\theta_{\pi\pi}$ (a) for Q = 0 pairs ($\pi^+\pi^-$) (139×9 pairs) (b) for | Q | = 2 pairs ($\pi^\pm\pi^\pm$) (139×6 pairs).

We can assume that most of the $8\pi$ events go by the reaction $\bar{p} + p \rightarrow \pi^+ + \pi^- \omega + \omega$, and that if a four-pion resonance really existed, a big fraction of the $8\pi$ events would go by this resonance ($\bar{p} + p \rightarrow 4\pi + X^0$ and $X^0 \rightarrow 4\pi$). We base this assumption on the big difference between the value of the cross section of the reaction $\bar{p} + p \rightarrow 3\pi^+ + 3\pi^- + 2\pi^0$ ($1.05 \pm .2$ mb) and that of $\bar{p} + p \rightarrow 4\pi^+ + 4\pi^-$ ($.025 \pm .01$ mb) (Table V). A statistical calculation would give a ratio of 7 for the rate of the first reaction over the second one; we find here a ratio of $40 \pm 10$. This assumption can explain also the absence of $\rho$ mesons in the $8\pi$ events.

## VI. SUMMARY AND CONCLUSION

Let us make a summary of the few interesting findings of this work. The cross section of the three analyzed reactions are found to

$$(\bar{p} + p \rightarrow 3\pi^+ + 3\pi^-) = 1.16 \pm .1 \text{ mb},$$

$$(\bar{p} + p \rightarrow 3\pi^+ + 3\pi^- + \pi^0 = 1.80 \pm .25 \text{mb},$$

$$(\bar{p} + p \rightarrow 3\pi^+ + 3\pi^- + 2\pi^0) = 1.05 \pm .25 \text{mb}.$$

The difference between the cross section of the reaction $\bar{p} + p \rightarrow 3\pi^+ + 3\pi^- + 2\pi^0$ and the reaction $\bar{p} + p \rightarrow 4\pi^+ + 4\pi^-$ ($.025 \pm .01$ mb) (see Table V) suggests that the first one would go through resonances whose decay includes neutral pions. This can be the known three-pion resonance or a yet undetermined four-pion resonance. The angular distributions are symmetrical for all three types of events (Figs. 14, 15, 16). This result is in contrast with the asymmetry found by Maglić et al.[20] in the reactions $\bar{p} + p \rightarrow 2\pi^+ + 2\pi^- + n\pi^0$ at the same energy. But because the ratio of the number of cloud pions to the number of core pions is smaller, Koba-Takeda theory would predict a smaller asymmetry, which could be masked in our case.

The existence of the $\omega$ meson ($I = 0$, three-pion resonance at 780 Mev) is further confirmed. With the hypothesis of G-parity conservation in the decay process (strong decay), the $\omega$ spin and parity is found to be $1^{--}$ by the Dalitz plot method. Even with the hypothesis of nonconservation of G parity in the decay process (electromagnetic decay), the $1^{--}$ spin and parity assignment is strongly suggested by the small values of the ratios $R(\omega \rightarrow 4\pi / \omega \rightarrow \pi^+ + \pi^- + \pi^0)$ and $R(\omega \rightarrow \text{neutral} / \omega \rightarrow \pi^+ + \pi^- + \pi^0)$. These results agree very well with those of Stevenson et al.[24]

The mass of the $\omega$ meson form $\bar{p}$-p annihilation seems to be $780 \pm 5$ Mev. That from pion-nucleon or nucleon-nucleon interactions seems to be 764 Mev (with about 5 Mev uncertainty). This difference in mass can be due to a systematic error in the track reconstruction

of the bubble chamber, or an influence of the presence of the nucleon in the final states.

Neither we nor Maglić et al. have observed in the $\bar{p}$ - p annihilation the T=0 three-pion resonance at 550 Mev reported by Pevsner et al.[30] and Bastien et al.[30]

The distribution of the neutral four-pion effective mass $M_4$ shows a suggestive but inconclusive peak at 1.04 Bev (Fig. 24).

The two-pion effective-mass distributions at 6 $\pi$ events show a big difference between the $|Q| = 2$ or like-pion pairs and the $Q = 0$ or unlike-pion pairs at the low-value region of $M_2$ (Fig. 27). At this region ($M_2$ between 280 and 460 Mev) the distribution for like-pion pairs is above that obtained from phase-space calculation, and the one for unlike pion pairs is well below. This result is similar to the result from the analysis of $\bar{p} + p \rightarrow 2\pi^+ + 2\pi^- + \pi^0$ at rest,[34] and different from the one of the analysis of $\bar{p} + p \rightarrow 2\pi^+ + 2\pi^- + \pi^0$ at the same energy.[17] We wonder if the similarity and difference may reflect the similarity and difference in the average energy available for one pion (382 Mev in our case, 396 Mev for 5 $\pi$ events at rest, and 458 Mev for 5 $\pi$ events at 1.61 Bev/c).

We tentatively attribute the difference of $M_2$ distributions in the low-value region, at least at present, to the Bose-Einstein effect on the pion as suggested by Goldhaber et al.[37] But no calculations have been done for the $\bar{p} + p \rightarrow 3\pi^+ + 3\pi^-$ reaction.

The ratio $R(\rho \rightarrow \pi^\pm + \eta,\ \eta \rightarrow \pi^+\pi^-\pi^0 / \rho^\pm \rightarrow \pi^\pm\pi^0)$ has been determined to be 1.2±2.0%. This small ratio agrees with the $0^{-+}$ assignment for spin, parity, and G parity of the $\eta$ meson but cannot rule out the possibility of $1^{--}$ assignment.

Table VIII gives the upper limits of some decay rates of the $\rho$ and $\omega$ mesons determined in this experiment.

In this work, we concern ourselves mostly with the search for multi-pion resonances and the determination of their quantum numbers. We feel that the real behavior of the antiproton-proton annihilation process will not be understood until all the multipion resonances and their quantum numbers are known. Many theories on $\bar{p}$-p annihilations

Table VIII. Upper limits of some decay rates of the $\omega$ and $\rho$ mesons

| Ratio | Upper limit |
|---|---|
| $R(\rho^0 \rightarrow 2\pi^+ 2\pi^- / \rho^0 \rightarrow \pi^+\pi^-)$ | 0.02 |
| $R(\rho^\pm \rightarrow \pi^\pm\pi^-\pi^+\pi^0 / \rho^\pm \rightarrow \pi^\pm\pi^0)$ | 0.05 |
| $R(\omega \rightarrow \text{neutral} / \omega \rightarrow \pi^+\pi^-\pi^0)$ | 0.5 |
| $R(\omega \rightarrow 4\pi / \omega \rightarrow \pi^+\pi^-\pi^0)$ | 0.17 |
| $R(\omega \rightarrow 2\pi^+ 2\pi^-\pi^0 / \omega \rightarrow \pi^+\pi^-\pi^0)$ | 0.01 |

do not include the multipion resonance states. The latest statistical model that includes all the known resonances is given by Kalbfleisch.[38] It gives a good prediction of the rate of diverse $\bar{p}$-p annihilation processes. But it is semi-empirical and still needs a large interaction volume ($\Omega = 4\,\Omega_0$. where $\Omega_0 = (4\pi/3)\,(\hbar/m_\pi C^3)^2$. Also no theory has ever included the spins of the proton and of the antiproton. On the experimental side Lannutti et al., by studying the double scattering of antiprotons in hydrogen, have shown that antiprotons can be polarized.[39] The annihilation of polarized antiprotons on hydrogen has been studied in a preliminary way.[40] It would be interesting to push this study forward, because it may give new understanding of the antiproton-proton annihilation process.

## ACKNOWLEDGMENTS

Thanks are due to all the many people who contributed to the execution of this experiment.

I want to thank Professor Luis W. Alvarez, not only because his foresight and interest have made this experiment possible but also because he has always provided me with help and advice of many kinds. I thank Professor M. Lynn Stevenson for his guidance and interest from the beginning of this antiproton experiment three years ago. I want also to thank Dr. Murray Gell-Mann for many theoretical discussions, Dr. Bogdan Maglić and Dr. Gerald Lynch for experimental discussions and advice, and Professor Arthur Rosenfeld for advice on the use of PANG and KICK programs.

Many people contributed to the operation of this Bevatron beam. The beam was designed by Dr. Stevenson, Dr. Philippe Eberhard, and Dr. George Kalbfleisch. The setup and operation of the beam was performed by the designers and by Dr. Janice Button, Dr. Joseph Lannutti, Dr. Gerald Lynch, Dr. Bogdan Maglić, and Dr. Morris Pripstein. Dr. John Poirier, Dr. Sherwood Parker, and Dr. Keith Hinrichs and other members of the Moyer group set up and operated the electronic equipment that was essential to the beam operation. The bubble chamber crews, under the direction of Messrs. J. Donald Gow and Robert Watt, kept the chamber in good operating condition. They also assisted with the vacuum system and high-voltage spectrometers of the beam. Mr. Mario Carota and Mr. George Edwards helped with the engineering and installation of the beam. The scanning personnel, under the direction of Dr. Hugh Bradner and Dr. Margaret Alston, were helpful is assisting with the beam development and operation as well as with the scanning of the film. The Bevatron crews, under the direction of Dr. Edward J. Lofgren, gave us the desired beam spill so essential to good bubble chamber pictures.

I thank Dr. Gerald Lynch and Dr. Joseph Lannutti for the results obtained from the master-list programs, and Dr. George Kalbfleisch

and Mr. Mark Horowitz for the calculation of the mass distribution of the pairs of particles for the Lorentz-invariant phase space. Mr. Joe Requa deserves thanks for his enormous help at various stages of the analysis, especially in the sketching of the events.

I wish to thank Dr. Cecil Tate for his assistance in the coding of the event-type control sub program of the KICK program for this experiment. I thank Mr. David Johnson for the development of the EXAMIN system. Mr. Leonard Reed and Mr. Cecil Draper set up the event-type control for the PANG program. Messrs. Robert Harvey, Cecil Draper, Tom Tonnison, and others of our computer staff were helpful in expediting the running of these programs.

I want to thank the Agency for International Development for a scholarship.

This work was done under the auspices of the U.S. Atomic Energy Commission.

# APPENDIX

## 1. G Parity and Strong Decay of the Heavy Mesons with Zero Strangeness, as Proposed by the "Eightfold Way" Theory

In the "eightfold way" theory, a heavy meson with strangeness S=0 can be represented by a definite state of $\bar{N}N$ (or $\bar{\Lambda}\Lambda$). It has been shown that for such a state the G parity is given by $G = (-1)^{s+\ell+I}$, where s, $\ell$, I represent respectively the spin, angular momentum, and I spin of the $\bar{N}N$ state.[41] Table IX gives the characteristics of the $\bar{N}N$ states representing the mesons with S=0 proposed in the eightfold way theory, and the resulting G parity.

Table IX. Characteristics of $\bar{N}N$ states representing some proposed heavy mesons and their G parities

| Meson | I spin | Spin and parity | $\bar{N}N$ | G parity |
|---|---|---|---|---|
| $\pi$ | 1 | $0^-$ | $^1S_0$ | -1 |
| $\rho$ | 1 | $1^-$ | $^3S_1$ | +1 |
| $\omega$, B | 0 | $1^-$ | $^3S_1$ | -1 |
| $K^0$, A | 0 | $0^-$ | $^1S_0$ | +1 |
| $\pi'$ | 1 | $0^+$ | $^3P_0$ | -1 |
| $\rho'$[a] | 1 | $1^+$ | $^3P_1$ | -1 |
| $\omega'$, $B'$[a] | 0 | $1^+$ | $^3P_1$ | +1 |
| $\chi^{0'}$, $A'$ | 0 | $0^+$ | $^3P_0$ | +1 |

(a) $\rho'$, $\omega'$ and $B'$ can be represented by either the $^3P_1$ or $^1P_1$ state, but Gell-Mann prefers the first state for "field theory" reasons (private communication).

The G parity of a state of n pions is given by $G = (-1)^n$. Since in strong interactions G parity is conserved, a heavy meson with G parity even can decay strongly into only an even number of pions (2, 4, 6, etc.), and a heavy meson with G parity odd can decay strongly into only an odd number of pions. The exceptions are that a $\chi^0$ or A meson cannot decay into two pions because of Bose statistics and conservation of intrinsic parity, also the $\pi'$ meson cannot decay into three pions for the same reasons.

## 2. Missing Energy and Missing Mass of the Events $\bar{p} + p \to 2\pi^+ + 2\pi^- + e^+ + e^- + \gamma$ When Mistaken as $\bar{p} + p \to 3\pi^+ + 3\pi^- + n\pi^0$

In many cases a six prong event has only four charged pions and a Dalitz pair. Most of the time this comes from the reaction $\bar{p} + p \to 2\pi^+ + 2\pi^- + \pi^0$ with $\pi^0 \to e^+ + e^- + \gamma$. For this reaction the energy- and momentum-conservation laws would give

$$\vec{P}_{\bar{p}} = \vec{P}_\gamma + \sum_{i=1}^{4} \vec{P}_i + \sum_{i=5}^{6} \vec{P}_i$$

and

$$E_{\bar{p}} + M_p = \sum_{i=1}^{4} \sqrt{(P_i^2 + M_\pi^2)} + \sum_{i=5}^{6} \sqrt{(P_i^2 + M_e^2)} + |P_\gamma| ,$$

where $\vec{P}_{\bar{p}}$, $E_{\bar{p}}$ is the momentum and energy of the antiproton, $M_{pr}$ the mass of the proton, $\vec{P}_1, \cdots, \vec{P}_4$ are the momenta of the four charged pions and $\vec{P}_5, \vec{P}_6$ are the momenta of the Dalitz pair.

By eliminating $P_\gamma$ we can deduce the relation

$$\left| \vec{P}_{\bar{p}} - \sum_{i=1}^{6} \vec{P}_i \right| = (E_{\bar{p}} + M_p) - \left( \sum_{i=1}^{4} \sqrt{(P_i^2 + M_\pi^2)} + \sum_{i=5}^{6} \sqrt{P_i^2 + M_e^2} \right) . \qquad (1)$$

We mistake the preceding event for a $\bar{p} + p \to 3\pi^+ + 3\pi^- + n\pi^0$ event only when the Dalitz pairs are very energetic (if not, we can recognize

them at the scanning table). In the case our track-reconstruction program (PANG) would give the same momentum $\vec{P}_5$ and $\vec{P}_6$ to the two electron prongs even if they were associated with pion mass.

If all six visible tracks are taken to be pions, the missing momentum and the missing energy are calculated according to

$$\overrightarrow{\Delta P} = \vec{P}_{\bar{p}} - \sum_{i=1}^{6} \vec{P}_i$$

and

$$\Delta E = (E_{\bar{p}} + M_p) - \left( \sum_{i=1}^{6} \sqrt{(P_i^2 + M_\pi^2)} \right) .$$

By the relation (1) we get

$$| \overrightarrow{\Delta P} | = (E_{\bar{p}} + M_p) - \left( \sum_{i=1}^{4} \sqrt{(P_i^2 + M_\pi^2)} + \sum_{i=5}^{6} \sqrt{(P_i^2 + M_e^2)} \right) ,$$

i.e., $| \Delta P | > \Delta E$ .

The square of the missing mass is given by the relation

$$MM^2 = (\Delta E)^2 - | \overrightarrow{\Delta P} |^2$$

There are two possibilities:

(a) for $\Delta E \geq 0$ ,
then $MM^2 < 0$,
and the missing mass is imaginary;

(b) For $\Delta E < 0$ ,
the missing mass can be real.

Conclusion: When we mistake $\bar{p} + p \rightarrow 2\pi^+ + 2\pi^- + \pi^0$ event with $\pi^0 \rightarrow e^+ + e^- + \gamma$ for a $\bar{p} + p \rightarrow 3\pi^+ + 3\pi^- + n\pi^0$ event, then either the missing energy is negative or the missing mass is imaginary.

## 3. Study of the Possible Errors of the Track-Reconstruction Program (PANG) in the 72-inch Bubble Chamber

Figure 6 shows that our experimental $\chi^2$ distribution of the reaction $\bar{p} + p \rightarrow 3\pi^+ + 3\pi^-$ (which when fitted has 4 constraints) agrees with the theoretical curve only if we multiply the scale of the latter by a factor of 3. We observe the same effect on the elastic scattering events $\bar{p} + p \rightarrow \bar{p} + p$ (also four constraints). This could suggest that the major cause of the discrepancy between the observed distribution and the theory is due to underestimated uncertainties in the measured variables. But the typical uncertainties would be underestimated by a ratio of $\sqrt{3} = 1.73$, which seems high. Some systematic errors could exist in our track-reconstruction program (PANG)

To check the PANG program, thorough tests have been done under the direction of Dr. Gerald Lynch.[42] The main idea is to put a grid in the 72-inch bubble chamber. The position of the grid is carefully measured. We took pictures, and measured and processed them through the PANG program in the usual way. By comparing the reconstructed grid and the real one, precise determinations can be made of the optical constants of the PANG program (positions and direction of the cameras, positions and direction of the lenses, etc.). Some slight discrepancies have been found.[42] Also the magnetic field at different points in the 72-inch bubble chamber has been more carefully measured. All these changes have been put into a new PANG program.

After processing with this new program, the $\chi^2$ distribution of the reaction $\bar{p} + p \rightarrow 3\pi^+ + 3\pi^-$ still differs from the theoretical curve by a factor of 3. Also, the fitted values remain about the same.

The same tests also showed that the antiproton pictures bear possible optical distortion due to the plastic vacuum ports (thickness = 1.5 inches) which were not adequately flat. In December 1960, these windows were changed to glass. The 72-inch chamber has

has been exposed to a $\pi^-$ beam in 1961 and the $\chi^2$ distribution of the $\pi^- + p \rightarrow \pi^- + p + \pi^+ + \pi^-$ events (four constraints) now differs from the theoretical curve by a smaller factor of 1.8.[42]

We conclude that our track-reconstruction program does not have large systematic errors, although the uncertainties of measured variable are underestimated, but the antiproton pictures have some additional optical distortion owing to the plastic vacuum ports. This effect would increase the uncertainties in some measured variables.

## References and Footnotes


1. M. Gell-Mann, The Eightfold Way: A Theory of Strong Interaction Symmetry, California Institute of Technology Synchroton Laboratory, Report No. CTSL 20 (1961); Symmetries of Baryons and Mesons, Phys. Rev. (to be published)
2. S. Sakata, Progr. Theoret. Phys. (Kyoto) 16, 686 (1956).
3. J. J. Sakurai, Ann. Phys. 11, 1 (1960); Nuovo cimento 16, 388 (1960). See also G. Breit, Phys. Rev. 120, 287 (1960); Y. Ne'eman, Nuclear Phys. (in press); A. Salam and J. C. Ward, Nuovo cimento (in press).
4. M. Ikeda, S. Ogawa and Y. Ohnuki, Progr. Theoret. Phys. 22, 715 (1959); Y. Ohnuki, Proceedings of the 1960 Annual International Conference on High Energy Physics at Rochester (Interscience Publishers, New York, 1960); Y. Yamaguchi, Progr. Theoret. Phys. Suppl. No. 11 (1959); J. Wess, Nuovo cimento 10, 15 (1960); Shigeo Minami, Heavy Mesons and Hard Core in Nuclear Force, Preprint, Department of Physics, Osaka City University, Osaka; H. P. Durr, W. Heisenberg, H. Mitter, S. Schneider, and K. Yamaguchi, Naturforsch. 14a, 441 (1959).
5. G. Chew, R. Karplus, S. Gasciorowicz and F. Zachariazen, Phys. Rev. 110, 265 (1958); P. Federbush, M. L. Goldberger, and S. B. Treiman, Phys. Rev. 112, 642 (1958); W. R. Frazer and J. R. Fulco, Phys. Rev. 117, 1609 (1960); See also J. Bowcock, N. Cottingham, and D. Lurie, Nuovo Cimento 16, 918 (1960).
6. Y. Nambu, Phys. Rev. 106, 1366 (1957).
7. P. Eberhard, M. L. Good, and H. K. Ticho, A Separated 1.17-Bev/c $K^-$-Meson Beam, UCRL-8878, Aug. 1959.
8. J. Button, P. Eberhard, G. R. Kalbfleisch, J. E. Lannutti, G. R. Lynch, B. C. Maglić, M. L. Stevenson, and N. H. Xuong, Phys. Rev. 121, 1788 (1961); George R. Kalbfleisch, A study of K Meson in Antiproton-Proton Annihilation (Thesis) UCRL-9597, March 1961.

9. C. Combes, B. Cork, W. Galbraith, G. Lambertson, and W. Wenzel, Phys. Rev. 112, 1303 (1958).

10. Gerald R. Lynch, Results from the 1.63-Bev/c Antiproton Master List, Alvarez Physics Memo No. 236, November 1960.

11. Hugh Bradner, Bubble Chambers, UCRL-9199, May 1960; J. V. Franck, "Franckenstein," A Semiautomatic Measuring Projector for Bubble Chamber Film, to be submitted to Rev. Sci. Instr.

12. William E. Humphrey, A Description of the PANG Program, Alvarez Group Memo 111, Sept. 18, 1959, and Memo 115, Oct. 25, 1959; A. H. Rosenfeld, Digital-Computer Analysis of Data from Hydrogen Bubble Chambers at Berkeley, In Proceedings of the International Conference on High-Energy Accelerators and Instrumentation, CERN 1959 CERN, Geneva, 1959).

13. Arthur H. Rosenfeld and James N. Snyder, Digital-Computer Analysis of Data from Bubble Chambers. IV. The Kinematic Analysis of Complete Events (UCRL-9098, Feb. 1960) Rev. Sci. Instr. (to be published); J. P. Berge, F. T. Solmitz, and H. Taft, Digital-Computer Analysis of Data from Bubble Chambers. III. The Kinematical Analysis of Interaction Vertices (UCRL-9097, March 1960) Rev. Sci. Instr. (to be published).

14. G. R. Lynch, Revs. Modern Phys. 33, 395 (1961). The process $\bar{p}+p \rightarrow \pi^+ + \pi^- + \pi^0$ is being studied. The cross section quoted here is just a preliminary result. Also Nguyen-Huu Xuong, G. R. Lynch and C. K. Hinrichs, Phys. Rev. 124, 575 (1961).

15. The EXAMIN program is described by D. Johnson of our programming staff in Alvarez Group Memo 271, March 1961.

16. T. Elioff, L. Agnew, O. Chamberlain, H. Steiner, C. Wiegand, and T. Y. Ypsilantis, Phys. Rev. Letters 3, 285 (1959); R. Armenteros, C. H. Coombes, B. Cork, G. R. Lambertson, and W. Wenzel, Phys. Rev. 119, 2068 (1960); C. Keith Hinrichs, Charge-Exchange Production of Antineutrons and Their Annihilation in Hydrogen (Thesis) UCRL-9589.

17. J. Button, G. R. Kalbfeisch, G. R. Lynch, B. C. Maglić, A. H. Rosenfeld, and J. L. Stevenson, Pion-Pion Interaction in the Reaction $\bar{p}+p \rightarrow 2\pi^+ + 2\pi^- + n\pi^0$ Phys. Rev. (to be published) (UCRL-9814, -Dec. 1961). The cross sections are only preliminary results.

18. Robert Foulks (Lawrence Radiation Laboratory), private communication.

19. A. Pais, Phys. Rev. Letters 3, 242 (1959).

20. B. C. Maglić, G. R. Kalbfeisch, and M. L. Stevenson, Phys. Rev. Letters 7, 137 (1961).

21. Z. Koba and G. Takeda, Progr. Theoret. Phys. (Kyoto) 19, 269 (1958).

22. The $M_3$ resolution is defined as the half width at the half maximum of the Gaussian ideogram obtained by using the uncertainty $\delta M_3$ and a fixed central value.

23. B. C. Maglić, L. W. Alvarez, A. H. Rosenfeld, and M. L. Stevenson, Phys. Rev. Letters 7, 178 (1961); N. H. Xuong and G. R. Lynch, Phys. Rev. Letters 7, 327 (1961); A. Pevsner, R. Kraemer, M. Nussbaum, C. Richardson, P. Schlein, R. Strand, T. Toohig, M. Block, A. Engler, R. Gessaroli, and C. Meltzer, in Proceedings of 1961 Conference on Elementary Particles, Aix en Provence; E. L. Hart, R. I. Louttit, D. Luers, T. W. Morris, W. J. Willis and S. S. Yamamoto, Multiple Meson Production in Proton-Proton Collisions at 2.85 Bev, Phys. Rev. (to be published).

24. R. Dalitz, Phil. Mag. 44, 1068 (1953). See also E. Fabri, Nuovo cimento 11, 479 (1954).

25. M. L. Stevenson, L. W. Alvarez, B. C. Maglić, and A. H. Rosenfeld, Phys. Rev. 125, 687 (1962). See also N. H. Xuong and G. R. Lynch, Phys. Rev. Letters 7, 327 (1961).

26. We are aware of the difficulty of making this subtraction. Some of the triplets in the peak region which are assumed to be in the

background may have the same quantum number as the $\omega$ meson. If this is true, the background subtraction should overemphasize the effect, no matter which spin and parity the particle has.

27. H. P. Duerr and W. Heisenberg (Max-Planck Institut, Munich), The Quantum Numbers of the $\omega$ Meson (preprint).

28. G. F. Chew, Phys. Rev. Letters 4, 142 (1960).

29. A. R. Erwin, R. March, W. D. Walker, and E. West, Phys. Rev. Letters 6, 628 (1961); E. Pickup, D. K. Robinson, and E. W. Salant, Phys. Rev. Letters 7,192 (1961); D. Carmony and R. Van de Walle, Phys. Rev. Letters 8, 73 (1962). These articles give a more complete reference to earlier publications on this subject.

30. A. Pevsner, R. Kraemer, M. Nussbaum, C. Richardson, P. Schlein, R. Strand, T. Toohig, M. Block, A. Engler, R. Gessaroli, and C. Meltser, Phys. Rev. Letters 7, 421 (1961); P. L. Bastien, J. P. Berge, O. I. Dahl, M. Ferro-Luzzi, D. H. Miller, J. J. Murray, A. H. Rosenfeld, and M. B. Watson, Phys. Rev. Letters 8, 114 (1962); D. C. Carmony, A. Rosenfeld, and R. Van de Walle, Phys. Rev. Letters 8, 117 (1962).

31. G. F. Chew and Steven C. Frautschi, Phys. Rev. Letters 8, 41 (1962); Phys. Rev. Letters 7,395 (1961). Also C. Lovelace (preprint).

32. A. Rosenfeld, D. Carmony, and R. Van de Walle, Phys. Rev. Letters 8, 293 (1962).

33. S. Glashow and J. Sakurai, private communication.

34. G. Goldhaber, W. B. Fowler, S. Goldhaber, T. F. Hoang, T. E. Kalogeropoulos, and W. M. Powell, Phys. Rev. Letters 3, 181 (1959). See also T. H. Hoang and J. Young, Covariant Phase-Space Factors for Reactions Involving Four to Six Secondary Particles, UCRL-9050, Jan. 1960.

35. G. Kalbfleisch, Lorentz-Invariant Phase-Space Distribution for the Effective Moss of Two Particles, Alvarez Physics Note No. 234 November 17, 1960.

36. W. Lee, W. Chinowsky, G. Goldhaber, and S. Goldhaber, Bull. An. Phys. Soc. 6, 522 (1961).

37. G. Goldhaber, S. Goldhaber, W. Lee, and A. Pais, Phys. Rev. 120, 300 (1960).

38. George R. Kalbfleisch, A Two-Parameter Statistical Model, UCRL-10024, Jan. 1962.

39. J. Lannutti, G. Lynch, B. Maglić, M. L. Stevenson, and Nguyen-Huu Xuong, Double Scattering of Antiprotons in Hydrogen, in Proceedings of the 1960 Annual International Conference on High Energy Physics at Rochester (Interscience Publishers, Inc., New York, 1960).

40. Nguyen-Huu Xuong, Annihilation of Polarized Antiprotons in Hydrogen, Bull. Am. Phys. Soc. 7, 298 (1962).

41. T. D. Lee and C. N. Yang, Nuovo cimento 3, 749 (1956).

42. G. R. Lynch, Constants in the PANG Program for the 72-inch Chamber, Alvarez Physics Memo 325, August 1961.